Early studies on a novel phosphoinositide 3-kinase p110β isoform, and its localisation

Sindre Hole

December 2020

This thesis is submitted in partial fulfilment
of the requirements for the degree of
Master of Science.

Department of Biological Sciences
Faculty of Mathematics and Natural Sciences
University of Bergen

Acknowledgements

The work presented in this thesis was carried out at the Department of Biological Sciences, University of Bergen, in the period of January to December 2020.

I would like to thank my wonderful supervisor Aurélia Lewis. I can only hope that I said enough thanks, and thank you's in the lab, as you were always willing to help if there was anything. With a smile, and your reassuring nature, I never felt dissuaded from knocking, or writing to you if I was wondering about anything. I would also like to thank you for being especially amazing during this less than grand year. Making sure that I had a lab to come back to as soon as possible, and making the best of the situation.

I would also like to thank my co-supervisor Diana Cornelia Turcu. A title unfitting, as you were just as much help, if not more so, than anyone else in the laboratory. Your near endless supply of patience is something i can only hope to be able to emulate. Without you I would never have been able to even start my master's. I'm not good with words in general, much less words of gratitude, so I will just say: thank you.

I would also like to thank Sandra Ninzima, for helping anytime I needed, and giving me a solid foundation for how to conduct nuclear extractions. I would also like to thank Andrea Morovicz, for being my confidant of secrets. Both of you made me feel more like a member of the team, that a student, so thank you. I would also like to thank Andreas Midlang, adn Elisabeth Lind, it is good having someone you know in the lab, shame that we started a semester of, and got lockdown, I would have liked to be able to talk, and joke around more. Thank you to the rest of the NucReg team, and beyond for a wonderful work-environment.

My most sincere gratitude to all my friends, I can't list you all, but you know who you are. Of the ones I can list I would like to thank Dan Martin, you have been there with me, on, and off since, what 4th grade now? I truly appreciated being able to totally forget about school, and just talk about nothing. Shame we were not able to talk more during this year, real life sure is a pain. I would also like to thank Oskar Leirvåg, and Ingrid Johansen, for dragging me out of my room to actually do something social every now and then. I would also like to thank my DnD group, you are all silly, loud, and fun. You know who you are, thanks.

Finally I would like to thank my family. My mom for calling near every other week, and letting me know again, and again how much I mean to you, and how proud you are, thank you. Also a thanks to my dad, you may not be quite as vocal as mom about things, but I know, I know.

Contents

Glossary

BCA Bicinchoninic Acid Assay

dATG Downstream ATG

DMEM Dulbecco's Modified Eagles' Medium

EST Expressed sequence tag

FBS Fetal Bovine Serum

GAP GTPase-activating proteins

NLS Nuclear Localisation Signal

PFA Paraformaldehyde

PI3K Phosphoinositide 3-kinase

PIP_3 phosphatidylinositol (3,4,5)-phosphate

PPIn Polyphosphoinositide

PtdIns phosphatidylinositol

P/S Penicillin-Streptomycin

PTEN Phosphatase and Tensin homolog deleted on chromosome ten

RIPA Radioimmunoprecipitation Assay buffer

RTK Receptor tyrosine kinase.

TAE Tris-Acetate-EDTA

SDS-PAGE Sodium Dodecyl Sulfate Polyacrylamide Gel Electrophoresis

TSL Transcript support level.

1 Abstract

Phosphoionositide 3-kinase (PI3K) is a family of enzymes that are part of the PI3K signalling pathway, which is one of the most often altered pathways in human cancer. The PI3K family is divided into three classes, were the class I produce phosphatidylinositol (3,4,5)-triphosphate (PIP_3), a secondary messenger that acts upon several pathways, and is linked to cancer. Of the four distinct isoforms of class I PI3K, the p110α, and p110β forms are ubiquitously expressed in all tissues. Most research has been conducted on p110α, due to the frequent observations of mutations in cancers. . Less research has been done on p110β but it has been shown to be exhibit oncogene characteristics when overexpressed. (Or last sentence: p110β has also been extensively shown to exhibit oncogene activity.)

Our group has observed different resolving patterns when probing western blots with antibodies targeting other sites of the p110β protein. The focus of this thesis was to investigate and explain this inconsistency.

During this study, the existence of the theoretical short form of p110β "Q68", became a plausible explanation. This theoretical form started from a start codon at amino acid number 555, and contained an insert of 15 bp, compared to canonical p110β. To validate the existence of the p110β isoform, the insert was targeted in a RT-PCR experiment. The theoretical ATG site for the short form was found to have a stronger Kozak sequence then the canonical ATG. The validity of the Q68's ATG to function as a start codon was tested by mutating either the canonical ATG or the short form ATG. Then expressing these mutants and observing if the associated bands of each inform was present or not.

In addition, during this thesis, Q68 was found to exhibit autophagy like patterning when overexpressed, tagged to EGFP.

p110β has been implicated in autophagy, but these studies are controversial, the possible existence of a p110β isoform may clear these findings.

2 Introduction

2.1 Phosphoionositide 3-kinase

Phosphoionositide 3-kinase (PI3K) is a family of kinases that produce polyphosphoinositides (PPIns); signalling molecules that are involved in a wide array of signalling pathways, by phosphorylation. These kinases have seen a large amount of focus over the last few years. This is mainly due to their direct involvement in human disorders, such as cancer and diabetes mellitus type 2. The kinases are part of the PI3K pathway, which regulates the levels of different PPIns.

2.1.1 Phosphatidylinositol, and its phosphorylated derivatives.

Phosphatidylinositols (PtdInss) is a glycerophospholipid that accounts for about 10-15% of all membrane phospholipids (Viaud et al. 2016). It consists of an inositol head group, mounted to a glycerol backbone through a phosphodiester bond. Two hydrophobic acyl chains are connected on the glycerol backbone (Figure 2.1). Phosphorylation can be done on the 3′, 4′, and 5′ hydroxyl groups in the inositol ring, each permutation making one of the seven PPIns. Phosphorylation of the 2′, and 6′ is hindered, likely by steric hindrance (Viaud et al. 2016).

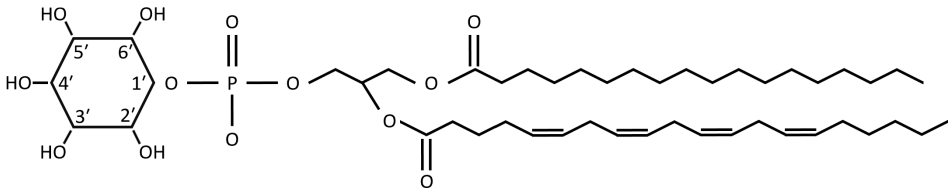

Figure 2.1: **Structural diagram of phosphatidylinositol.** The inositol headgroup is on the left with each hydroxyl group numbered. It is connected to the glycerol backbone with a phosphodiester bond. With ester bonds connecting the hydrophobic fatty acid chains (C18:0/C20:4) to the glycerol. Different PI3K can phosphorylate the hydroxyl groups on the 3′ positions.

The PPIns are categorised into three groups: the mono-phosphorylated (*PtdIns3P*, *PtdIns4P*, and *PtdIns5P*), the di-phosphorylated (*PtdIns(3,4)*P_2, *PtdIns(3,5)*P_2, and *PtdIns(4,5)*P_2), and one tri-phosphorylated (*PtdIns(3,4,5)*P_3). Distribution between these PPIns, and the PtdIns is not equal, with 80% of the total population being the non-phosphorylated PtdIns; with PtdIns4P, and PtdIns(4,5)P_2 making up about 10%, and

the remaining forms not representing more than 1-2% of the total PPIn population (Viaud et al. 2016).

These lipids function as secondary messengers for several different cellular processes. These include, but are not limited to autophagy, intracellular trafficking, cytokinesis, autophagosome maturation, cell survival, proliferation and motility. They can directly interact with protein domains such as PH (Plekstrin Homology), FYVE (Fab-1, YGL023, Vps27, and EEA1), PX (phox) or the ENTH (Epsin N-Terminal Homology) domains. The synthesis of PPIns is activated or inhibited by a variety of stimuli (Hormones, growth factors, adhesion molecules, chemoattractants, stresses, etc.), in order to create membrane territories, containing specific PPIns that then recruit specific signalling proteins to control different cellular events (Viaud et al. 2016).

2.1.2 PI3K's, and the PI3K pathway

Phosphorylation of the 3′ OH groups on the inositol headgroup of PtdIns and PPIns is done by the kinases in the PI3K family (Vanhaesebroeck and Waterfield 1999). This family is divided into three classes: I, II, and III. Class I consists of a group of heterodimers, made up of a catalytic subunit, and a regulatory subunit. Class I PI3Ks produce the tri-phosphorylated phosphatidylinositol (3,4,5)-triphosphate (PIP_3) from their substrate phosphatidylinositol (4,5)-bisphosphate (PtdIns(4,5)P_2) (Figure 2.2). Class I is further divided into Class IA, and IB. Class IA consists of the catalytic subunits: p110α, encoded by the gene *PIK3CA*; p110β, *PIK3CB*; and p110δ, by *PIK3CD*. The regulatory subunits are p85α, p55α, and p50α, encoded by *PIK3R1*; p85β, *PIK3R2*; p55γ, *PIK3R3*; and p87, by *PIK3R6*. Class IB only consists of the catalytic subunit p110γ encoded by *PIK3CG*; and its regulatory subunit p101, by the *PIK3R5* gene. The p110$\alpha$and p110β isoforms of PIK3 are expressed in all tissues, with p110γ, and p110δ only being found in immune cells (Vanhaesebroeck and Waterfield 1999, and Jean and Kiger 2014).

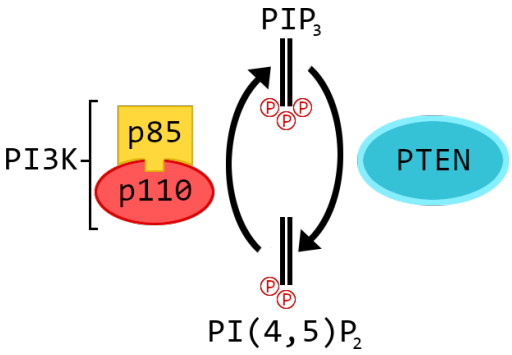

Figure 2.2: **Model of PI3K, and PTEN reactions on PtdIns(4,5)P_2, and PIP_3.** Model depicting the relationship between PI3K, and PTEN on PIP_3, and PtdIns(4,5)P_2, with arrows indicating the catalytic direction. The names p85, and p110 can be substituted for any of the other class I catalytic, and regulatory subunits.

As the class I PI3Ks are the main focus of this thesis class II, and III will be discussed in less detail. Class II are monomers that produce the mono-phosphorylated phosphatidylinositol 3-phosphate (PI3P), from PtdIns, and the di-phosphorylated PtdIns(3,4)P_2 from PtdIns4P. This class consists of three known catalytic isoforms: C2α, encoded by *PIK3C2A*; C2β, *PIK3C2B*; and C2γ, *PIK3C2G*. (Posor, Eichhorn-Grünig, and Haucke 2015, and Jean and Kiger 2014). Class III are heterodimers only known to produce PtdIns3P from PtdIns. (Leevers, Vanhaesebroeck, and Waterfield 1999). The heterodimer consists of the catalytic unit vacuolar protein sorting 34 (Vps34), encoded by *PIK3C3*; and its corresponding regulatory unit vps15, encoded by *PIK3R4* (Backer 2008, and Jean and Kiger 2014). One of the primary functions of the Vps34/Vps15 complex is to promote autophagy (Jaber and Zong 2013, and Kihara et al. 2001). An activator of the Vps34/Vps15 complex is Rab5, a small GTPase. It has been found that p85α can bind to Rab5 and inhibits its activity (Chamberlain et al. 2004).

The PI3K pathway is a part of the more extensive PI3K/Akt/mTOR pathway. This pathway is initiated by binding between PIP_3 and Akt. PIP_3 binding to Akt activates it and increases cell differentiation, cell growth, survival, and proliferation. Phosphorylation of Akt is done by phosphoinositide-dependent protein kinase 1 (PDK1), and mammalian target of rapamycin (mTOR) complex 2 (Sarbassov et al. 2005).

Inhibition of PIP_3 is mainly regulated by Phosphatase and tensin homolog deleted on chromosome ten (named so due to frequently being lost from a region of chromosome 10q23 in a variety of human tumours (Li et al. 1997, Steck et al. 1997)) (PTEN) by dephosphorylating of PIP_3, back to PtdIns(4,5)P_2 (Figure 2.2); making it a direct antagonist to class I PI3K, negatively regulating PIP_3 production. PTEN is a well-established tumour suppressor (Hopkins et al. 2014).

2.1.3 p110α, and p110β history, and main properties

The two ubiquitously expressed class IA PI3Ks (p110α, and p110β) were discovered around the same time. (p110β) was discovered in 1993, only a year after p110α was established as a PI3K (Hiles et al. 1992, and Hu et al. 1993). Translated from different genes *PIK3CA*, and *PIK3CB*, and their individual mouse KO are embryonically lethal (Bi, Okabe, Bernard, Wynshaw-Boris, et al. 1999, and Bi, Okabe, Bernard, and Nussbaum 2002). Even though these proteins were first described as PI3K virtually at the same time, the knowledge base for these proteins has since become disproportionate, with p110α having received the most attention from the scientific community. The main cause of this is that p110α is often mutated in cancer, while p110β is not (Zhao and Vogt 2008). This is discussed further in section 2.3.

The two ubiquitously expressed class IA PI3Ks (p110α, and p110β) both contain the same domains (Figure 2.3). However the functions of some of these domains differ between some of the domains on these two proteins.

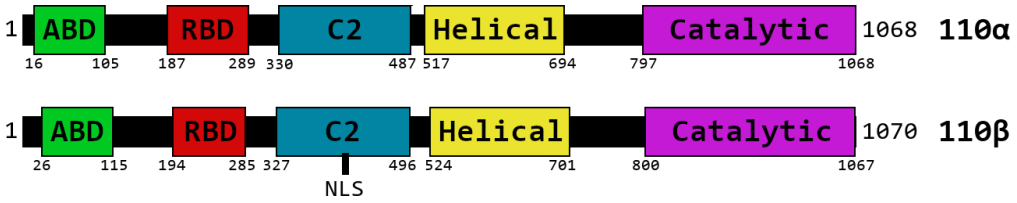

Figure 2.3: **A schematic model of both the p110αand p110β proteins.** The proteins are shown with numbered AA's from N-terminal to N-terminal for localisation of each domain. With the possible nuclear localisation signal (NLS) of p110βs localisation denoted in the C2 domain. Abbreviations: ABD - Adaptor Binding Domain, RBD - Ras Binding Domain.

The adaptor binding domain (ABD) is an N-terminal domain that functions as the binding site between the catalytic unit, and its regulatory subunit. The p85 subunit binds to p110 predominantly with a coiled-coil region, sandwiched between two SH2 domains, called the inter-SH2 domain. This binding is further stabilised by interactions with the catalytic subunits' helical, C2, and catalytic domains, to the regulatory unit. This binding stabilizes p110, by so far unknown mechanism(s), and inhibits its catalytic activity. The inhibition can be hindered, when p85 is bound to receptor tyrosine kinases (RTKs), by disturbing the interactions of p85 on the helical, C2, and catalytic domains of the catalytic subunit (Rodriguez-Viciana et al. 1996, and Burke and Williams 2015).

The ras binding domain (RBD) binds to the activators for class I PI3Ks, that act together

with the RTK signal on p85. For p110α these are RAS GTPase's. Interestingly p110β does not bind to RAS, but instead to proteins in the Rho subfamily of small GTPases (Fritsch et al. 2013). The C2 domain functions as a membrane targeting domain; binding to phospholipids, and regulates the localisation of the protein within the cell (Farah and Sossin 2012). Note that p110β has had proof of a NLS within this domain (Kumar et al. 2011). The helical domain is conserved among all the PI3Ks. Its role is not well understood, but it is likely involved in substrate presentation (*PIK helical domain - PRU00878* 2020). Lastly, the catalytic domain is a C-terminal catalytic domain, responsible for phosphorylation of PtdIns(4,5)P_2 to PIP_3.

The core downstream signalling is the same for all of the class I PI3Ks, those being Akt activation, Tec family tyrosine kinases, and guanine nucleotide exchange factors for small GTPases in the Rho and Arf families. Additionally, some downstream signalling pathways have been described that are p110β specific for the PI3K family (Bresnick and Backer 2019). Those pathways are "vesicular trafficking in the endocytic and autophagic systems" (Ciraolo et al. 2008, Jia et al. 2008, Dou, Chattopadhyay, et al. 2010, and Dou, Pan, et al. 2013); also several nuclear functions have been described for p110β. The nuclear functions that have been described for p110β so far are DNA repair and replication, and nuclear envelope maintenance, as well as chromosome segregation during mitosis (Kumar et al. 2011, Marqués et al. 2009, and Redondo-Muñoz, Josefa Rodríguez, et al. 2013, Redondo-Muñoz, Pérez-García, et al. 2015, and Silió, Redondo-Muñoz, and Carrera 2012).

For this thesis, its involvement in cancer, and autophagy are most central. Its connection in cancer development has been known about the longest. In fact, the discovery of the gene itself was directly tied to its binding to p85, and its sequence identity with p110α, resulting in this function of the protein being devised of at the same time as its discovery (Hu et al. 1993).

2.1.4 p110β, and autophagy

Autophagy is a membrane trafficking process that removes and recycles cellular components. Intracellular components are shuttled into the autophagosome, a bi-layered vacuole that fuses with a lysosome, containing a cocktail of enzymes that break down the contents of the autophagosome. This mechanism protects organisms against an array of pathologies, such as infections, cancer, neurodegeneration, ageing, and heart disease (Levine and Yuan 2005, Levine and Kroemer 2008). The initiation of autophagy in metazoans is regulated by PIP_3, and PI3P, produced by the class I, and class III PI3Ks (Viaud et al. 2016, Dou, Pan, et al. 2013). PIP_3 induces conformational changes in Akt, and this makes

it possible for other proteins to activate Akt, which will then, among other effects, inhibit autophagy (Huang et al. 2011). While PI3P initiates it. It was therefore recognised that class IA PI3Ks inhibited, while the class III PI3K, Vps34/Vps15, activated autophagy. However it has been found that p110β can function as a positive regulator of autophagy, independent of its catalytic activity (Dou, Chattopadhyay, et al. 2010).

In studies from Dou, Pan, et al. they describe the mechanism for how p110β is involved in autophagy. They found that p110β will, when the availability of growth factors becomes low, disassociate from its growth factor receptor signalling molecules, and instead bind to Rab5. This protects Rab5 from inhibiting signals and allows it to bind to the Vps34/Vps15 complex, and activate it (Dou, Chattopadhyay, et al. 2010, and Dou, Pan, et al. 2013).

Prior to these studies, the only known mechanism for initiating autophagy was based on nutrient availability. However, they discovered that the p110β mediated mechanism was dependent on growth factors instead, not the direct availability of nutrients (Dou, Pan, et al. 2013). As cells of higher order-multicellular life are often in nutrient-rich environments (Lum, DeBerardinis, and Thompson 2005), the ability to control autophagy despite the surrounding nutrient levels is a valuable control mechanism.

Of note is that the studies by Dou, Chattopadhyay, et al., and Dou, Pan, et al., are problematic for three reasons (Bresnick and Backer 2019). One: overexpression of active Rab5 could enhance autophagy independently of p110β, as Rab5 has been shown to inhibit the mTOR complex 1 (Flinn et al. 2010). Two: Rab5 has been shown to be expressed at 150 times more then p110β in vivo, (Schwanhäusser et al. 2011). p110β is therefore unlikely to have a noticeable effect on Rab5. Three: parts of the argument by Dou, Pan, et al., and relies on p85 being a Rab5 GAP, i.e. having a downregulating effect on the protein. This is not replicative under normal conditions; the only studies showing this connection between p85, and Rab5, have been done with p85 at 50 times the normal concentration (Dou, Pan, et al. 2013).

2.2 Nuclear PPIn, and p110β

2.2.1 Nuclear PPIn

The cytoplasmic roles of PPIn are well studied, the nuclear roles, however, are less understood. A significant reason for this is that while the nuclear localisation of PPIns was discovered in the 1980-90s (Cocco et al. 1987, Payrastre et al. 1992), their importance has only recently more evident (Fiume et al. 2019, Jacobsen et al. 2019). Independent nuclear

metabolism and signalling have also been observed. In fact, except for PtdIns(3,5)P_2, all PPIns have been detected in the nucleus (Lachyankar et al. 2000).

Multiple nuclear processes have been identified for PPin; mRNA processing, splicing and export, chromatin remodelling, transcription, and cell cycle progression (Davis, Lehmann, and Li 2015; Hamann and Blind 2018; Irvine 2003, Martelli et al. 2011; Musille, Kohn, and Ortlund 2013; Okada and Ye 2009; and Viiri, Mäki, and Lohi 2012). Nuclear PPIns have been found to interact with these processes mostly through interaction via polybasic regions (PBR), also called K/R rich motifs, but also in some cases through PH domains. The nuclear function of PIP_3 is still largely unknown. While some PIP_3 binding proteins have been identified within the nucleus, the function of how these proteins interact with PIP_3 is still not understood (Gavgani, Morovicz, et al. 2020).

2.2.2 Nuclear PIP_3 and p110β

Even though the function of nuclear PIP_3 is largely unknown, its presence, production, and breakdown are supported within the nucleus. A pool of PtdIns(4,5)P_2: PIP_3's precursor, has been observed (Osborne et al. 2001, Watt et al. 2002). The kinases that produce PtdIns(4,5)P_2 has been observed in the nucleus. p110β has also been observed in the nucleus, accounting for the production of PIP_3 (Kumar et al. 2011). In addition, the phosphatase PTEN, has also been observed within the nucleus (Gavgani, Morovicz, et al. 2020). These and additional findings all show that the cellular machinery necessary for the production, and regulation of PIP_3 is present within the nucleus.

Of the ubiquitously expressed class I PI3Ks, only p110β has been found to have a nuclear localisation. Meanwhile, the structural features that determine p110β nuclear localisation remain largely unknown. The p85β and a possible NLS in the C2 domain of p110β have been found to mediate its nuclear localisation (Kumar et al. 2011). Of note is that it is only the p85β regulatory subunit which facilitates this localisation, suggesting a possible control mechanism for nuclear localisation of p110β.

Interestingly our group has also shown that p110β has a nucleolar localisation. This suggests that p110β has a nucleolar role for the PI3K pathway that may contribute to tumour progression in endometrial cancer (Karlsson et al. 2016; and Gavgani, Karlsson, et al. 2019).

2.3 p110β and cancer

The PI3K pathway under normal circumstances is involved in cell differentiation, growth, survival; and proliferation (Viaud et al. 2016). All three of those points are involved in the hallmarks of cancer (Hanahan and Weinberg 2000, and Hanahan and Weinberg 2011). In fact, alterations to the PI3K pathway has been shown to lead to tumourigenesis and resistance to anticancer therapy (Yang et al. 2019). The hallmarks of cancer are a set of ten requirements for a cell to become cancerous, proposed by Hanahan and Weinberg. The requirements include; promote/sustain cell proliferation, migration, glucose transport and anabolism, cytoskeletal rearrangements, and angiogenesis. All ten points do not necessarily need to be fulfilled for a cell to become cancerous, although, most cancers observed, fulfil them all (Hanahan and Weinberg 2000, and Hanahan and Weinberg 2011).

The PI3K pathway is deregulated through several avenues: mutation or amplification of PI3K, activation of growth factor receptors, or oncogenes upstream of the pathway, or by loss or inactivation of PTEN (Yang et al. 2019).

The PI3K antagonist; PTEN is often mutated in cancers. Indeed it was discovered, and named, because of it (Steck et al. 1997). PTEN is regarded as a tumour suppressor gene. A statement supported by how loss or inactivation of PTEN is observed frequently, and in a wide array of cancers, including brain, breast, and prostrate cancer. (Yang et al. 2019). Interestingly it has been found that the inactivation of p110β, not the p110α PI3K isoform had a lessening effect on the prostate-cancer loss of PTEN phenotype for mice (Jia et al. 2008, and Berenjeno et al. 2012). It would therefore seem that at least prostrate cancer cells, rely more on p110β, than p110α for malignancy.

This is surprising as most cancerous mutations concerning PI3K, are found on p110α, not p110β (or p110γ, p110δ). Indeed about 30% of all carcinomas contain some mutation to the *PIK3CA* gene (Zhao and Vogt 2008). Upregulation of p110α activity has been shown to promote cell proliferation, migration, glucose transport and catabolism, cytoskeletal rearrangements, and angiogenesis (Yang et al. 2019, Fruman and Rommel 2014), all hallmarks of cancer development (except cytoskeletal rearrangement) (Hanahan and Weinberg 2000, Hanahan and Weinberg 2011, and Cosmic 2020). Giving p110α a vital role in the initiation, progression, and maintenance of cancer, as only a few mutations on p110α can fulfil several requirements for malignancy, and cancer.

Mutations in the *PIK3CB* gene, on the other hand, are rare. p110β is still involved in malignancy via other mechanisms. For example overexpression of p110β in its WT form have been shown to induce an oncogenic phenotype (Aoki et al. 2000, and Kang, Bader,

and Vogt 2005), in for example prostate, glioblastoma, and endometrial cancer (Thorpe, Yuzugullu, and Zhao 2015, and Karlsson et al. 2016). In addition it has been shown that p110β plays an important role in prostate, and breast cancer (Hill et al. 2010, and Dbouk et al. 2013). The mechanisms of how p110β is activated in cancer, and how it contributes to cancer development are not well understood (Yang et al. 2019).

Even though mutations on p110β are rare, several activating mutations have been reported (Bresnick and Backer 2019), such as the glutamic acid substitution to lysine on amino acid number 633 (E633K). This mutation, located in the helical domain, was first reported in the same cancer type as the co-inhibition study was conducted on, HER2-positive breast cancer (Kan et al. 2010). Interestingly this mutation showed a 150% catalytic effect compared to WT p110β when not in the presence of its regulatory unit. However, in the presence of p85, it had an equal catalytic effect as WT p110β in vitro. In contrast, when stably expressed in vivo, the expression was again higher for the E633K mutant. An increased association between p110β and the membrane may explain the increased activation caused by E633K. (Dbouk et al. 2013). In advanced prostate cancer, several p110α homologous mutations have been observed (Robinson et al. 2015). The D1067V activating mutation, located within the catalytic domain, has also been documented several times (Chang et al. 2016, Nakanishi et al. 2016, Pazarentzos et al. 2016, and Lasota et al. 2019).

2.4 Aims

The PI3K pathway is one of the most important pathways with regards to tumour development, and it is pivotal in several other cellular processes as well. The PIP_3 producing kinase p110β is not well understood when compared to the isoform p110α. In contrast to p110α, the p110β isoform was proven to not only be expressed in the cytoplasm but also the nucleus (Kumar et al. 2011). Our lab has also shown this localisation in a panel of endometrial cancer cell lines, including RL95-2, using an antibody raised against the N-terminal region of p110β (Gavgani, Karlsson, et al. 2019). Unexpectedly the resolving pattern was found to differ when using antibodies raised more towards the C-terminal end of the protein; showing additional bands in the nuclear fraction by western immunoblotting (Abcam, AA: 400-500; and Thermo Fisher, AA: 411-605) (unpublished data). This inconsistency suggested the existence of a possible additional isoform of p110β.

This thesis aimed to explore the possible existence of an additional p110β isoform, and to glean some of its possible functions, with the following aims:

- To determine the existence of a short p110β form.
- To clone the shorter p110β form, and determine its subcellular localisation.
- To determine the sub-cellular localisation of the short isoform within cancer cells.

3 Materials

Table 3.1: **Chemicals.**
ELG: electrophoresis grade, MBG: molecular biology grade. ANG: analysis grade. PG: practical grade.

Chemical	Abbrev.	Grade/ Purity	Supplier	Catalog number
2-Amino-2-hydroxymethyl-1.3-propanediol	Tris		Sigma-Aldreich®	1.10110
30% Acrylamide/Bisacrylamide			BioRad	161-0158
Agarose, SeaKem® LE	Agarose	ELG	Lonza	50004
Ampicillin	Amp		Sigma-Aldrich®	A9393
Calcium chloride	$CaCl_2$		Merck	1.02083
Dimethyl Sulfoxide	DMSO		Sigma-Aldrich®	472301
Ethanol	EtOH		Sigma-Aldrich®	600051
Ethidium Bromide	EtBr		Sigma-Aldrich®	E1510
Isopropanol	IPS		Kemetyl	600079
LB Agar		MBG	Sigma-Aldrich®	L2897
Magnesium Chloride	$MgCl_2$	ANG	Merck	1.05833
N,N,N',N'-tetramethylethane-1,2-diamine	TEMED		BioRad	161-0800
Polyoxyethylenesorbitanmonolaurate	Tween®20		Sigma-Aldrich®	P1379
Sodium chloride	NaCl	≥99.5%	Sigma-Aldrich®	31434N
2-[4-(2,4,4-trimethylpentan-2-yl)phenoxy]ethanol	Triton-X100			
3-hydroxy-4-(2-sulfo-4-[4-sulfophenylazo]phenylazo)-2,7-naphthalenedisulfonic acid sodium salt	Ponceau	PG	Sigma Aldrich	P3504

Table 3.2: **Antibodies used in Western Immunoblotting, and dilutions**
WB - Western Blotting

Antibody	Supplier	Catalogue #	Species	Dilution
α-Tubulin	Santa Cruz	8035	Mouse	1:20'000 WB
Lamin - A/C	Santa Cruz	376248	Mouse	1:10'000 WB
Mouse IgG HRP	Thermo Fisher	21040	Goat	1:10'000 WB
Rabbit IgG HRP	Thermo Fisher	21234	Goat	1:10'000 WB
p110β (C-8)	Santa Cruz	376641	Mouse	1:500 WB
p110β (1H9L37)	Thermo Fisher	703364	Rabbit	1:250 WB

Table 3.3: **Cell culture reagents**

Chemical	Abbrev.	Supplier	Catalog number
Dulbecco's Modified Eagles's Medium - high glucose	DMEM	Sigma-Aldreich®	D6429
Bovine Serum Albumin	BSA	SigmaAldrich®	A7906
100× Penicillin-Streptomycin	P/S	Merck	TMS-AB2-C
Trypsin-EDTA	Trypsin	Sigma-Aldreich®	T4049
Opti-MEM® (Minimal Essential Medium) Reduced-Serum Medium	Opti-MEM	Thermo Fisher Scientific	31985062
Foetal Bovine Serum	FBS	Sigma-Aldreich®	f7524

Table 3.4: **Cell lines and Bacteria**

Name	Description	Supplier
KLE	Human endometrium adenocarcinoma cells	Prof. HB Salvesen, Women's hospital, UIB
MFE	Human endometrium adenocarcinoma cells	Prof. HB Salvesen, Women's hospital, UIB
RL95-2	Human endometrial carcinoma cells	Prof. HB Salvesen, Women's hospital, UIB
HAP1	Near haploid human chronic myelogenous leukaemia cells	Dr H. Aksnes, UIB
HEK 293	Human embryonic kidney cells	Prof. M Ziegler, UIB
XL1-Blue	Supercompetent Cells (QuickChange)	Agilent

Table 3.5: **Equipment**

Name	Supplier	Software	Use
Epoch™ Microplate Spectro-photometer	BioTek	Gen5	DNA, RNA, and protein concentration measurement
NanoDrop™ 1000 Spectro-photometer	Thermo Fisher Scientific	ND-1000	DNA, and protein concentration measurement
Gel Doc™ EZ	BioRad	ImageLab	Agarose imaging
ChemiDoc™ XRS+	BioRad	ImageLab	Western blot imaging
Mini submarine electrophoresis unit	Hoefer		DNA electrophoresis
Sonication bath	VWR		Sonication
Leica DMI6000 B	Leica	Leica Application Suite	Fluorescent cell imaging

Table 3.6: **Primers**
Mutated ATG's to AAC are underlined.

Name	Sequence	Tm (°C)	Use
Forward Q68 Insert	5′-AAAATGGTGATGTTTGTTTTCCCT-TAGATTTACGACAGGATATG-3′	55	Insertion by SDM
Reverse Q68 Insert	5′-CTGTCGTAAATCTAAGGGAAAACA-AACATCACCATTTTTAAAAATC-3′	55	Insertion by SDM
Forward EcoRI pcDNA 110β	5′-AGTGTGGTGGAATTCTGAATGTGC-TTCAGTTTC-3′	50	Insertion by SDM, and Kozak introduction to p110β
Reverse EcoRI pcDNA p110β	5′-GTCGACTGCAGAATTCTTAAGATC-TGTAGTCTTTCCG-3′	50	Insertion by SDM, and Kozak introduction to p110β
Forward XhoI Q68	5′-GGACTCAGATCTCGAGATGGATCT-TATTTGGACTTTGC-3′	73	Cloning
Reverse EcoRI Q68	5′-GTCGACTGCAGAATTCTTAAGATC-TGTAGTCTTTCCG-3′	72	Cloning
Forward 1st ATG mutant	5′-GGAATTCTGAAACTGCTTCAGTTT-C-3′	65	Canonical p110β knockout
Reverse 1st ATG mutant	5′-GAAGCAGTTTCAGAATTCCACCAC-3′	67	Canonical p110β knockout
Forward 2nd ATG mutant	5′-AAAATGAAAACGATCTTATTTGGA-CTTTG-3′	66	Shortform p110β knockout
Reverse 2nd ATG mutant	5′-AAGATCGTTTTCATTTTCACACAG-3′	63	Shortform p110β knockout
Forward Insert 7591	5′-GTGATGTTTGTTTTCCC-3′	50	RT-PCR
Forward Insert 7495	5′-GGTGATGTTTGTTTTCCCTTAG-3′	57	RT-PCR
Forward Insert 8001	5′-GTTTGTTTTCCCTTAGATTTAC-3′	53	RT-PCR
Reverse Sequencing Primer	5′-CTTTAAGCCAGTTCAGAAGG-3′	56	RT-PCR

Table 3.7: **Kits, and reagents**

Name	Supplier	Use
Lipofectamine™ 3000 Reagent	Thermo Fisher	Transfection
QuikChange Site-Directed Mutagenesis Kit	Agilent Technologies	Site-directed mutagenesis
NucleoSpin® Gel and PCR Clean-up	Macherey-Nagel	Plasmid purification
NucleoSpin® Plasmid	Macherey-Nagel	Miniprep
SuperSignal® West Femto Maximum Sensitivity Chemiluminescence	Thermo Fisher	Western Blot Visualisation
SuperSignal® West Pico Chemiluminescence	Thermo Fisher	Western Blot Visualisation
NucleoSpin® Plasmid	Macherey-Nagel	Miniprep
NucleoSpin® Gel and PCR Clean-up	Macherey-Nagel	Plasmid purification
Nitrocellulose blotting membrane	GE Healthcare Life science	Western Blot

Table 3.8: **Vectors.**

Name	Template	Supplier	use
pEGFP-C2-p110β		Addgene	Localisation assessment
pEGFP-C1-Q68	PSG5 p110β	This study (S Hole)	Localisation assessment
pEGFP-C1-Empty		Addgene	Localisation assessment
pSG5-N-myc-hp110β WT		JM Backer (Albert Einstein College of Medicine, NY, USA)	pcDNA template
pcDNA p110β WT Kozak	PSG5-N-myc-hp110β WT	Diana C. Turcu	Canonical vs isoform knockout
pcDNA p110β 1st ATG mutant	pcDNA p110β WT Kozak	This study (S Hole)	Canonical vs isoform knockout
pcDNA p110β 2nd ATG mutant	pcDNA p110β WT Kozak	This study (S Hole)	Canonical vs isoform knockout

3.1 Standard solutions

3.1.1 Agarose gel electrophoresis

1× TAE Buffer
- 40 mM Tris
- 1 mM EDTA pH 8.0
- 20 mM Acetic acid

6× DNA sample buffer
- 30% Glycerol
- 0.025% Bromophenol Blue

3.1.2 Bacteria cultivation

LB agar
- 35 g/L LB Broth (Lennox; Sigma Aldrich)
- 15 g/L Agar
- 10 g/L Tryptone
- 5 g/L Yeast extract
- 5 g/L NaCl

LB medium
- 20g/L LB Broth (Lennox; Sigma Aldrich)
- 10 g/L Tryptone
- 10 g/L NaCl
- 5 g/L Yeast extract

Super Optimal Broth (SOC) medium
- 20 g/L Tryptone
- 5 g/L Yeast Extract
- 20 mM glucose
- 10 mM $MgSO_4$
- 10 mM $MgCl_2$
- 10 mM NaCl
- 2.5 mM g/L KCl

3.1.3 SDS-PAGE and Western Blotting

Resolving gel
- 8-12% acrylamide/bisacrylamide (37.5:1)
- 380 mM Tris pH 8.8
- 0.1% (v/v) SDS
- 0.1% (v/v) APS
- 0.06% (v/v) TEMED

Stacking gel
- 5% acrylamide/bisacrylamide (37.5:1)
- 125 mM Tris pH 6.8
- 0.1% (v/v) SDS
- 0.1% (v/v) APS
- 0.1% (v/v) TEMED

TBS-T
- 50mM Tris pH 7.5
- 150mM NaCl
- 0.05% Tween20 (100%)

Blocking buffer (Western Blot)
- 7% (w/v) powdered milk (1% fat) in TBS-T

Running buffer
- 25 mM Tris
- 192 mM glycine
- 0.1% (w/v) SDS
- pH 8.3

Transfer buffer
- 25 mM Tris
- 192 mM Glycine
- 20% (v/v) methanol
- pH 8.3

5× Sample buffer
- 10% SDS
- 500 mM DTT
- 50% Glycerol
- 250 mM Tris-HCl
- 0.5% bromophenol blue dye
- pH6.8

PFA solution
- 3.7% Paraformaldehyde in Phosphate-Buffered Saline (PBS)

4 Methods

4.1 Cell work

4.1.1 Cultivation

Cell lines were grown, and cultivated in Dulbecco's Modified Eagles' Medium (DMEM), with 10% fetal bovine serum (FBS), and 1% penicillin-streptomycin (P/S). Cells were cultured in 10 cm round cell culture dishes, at 37℃ with 5% CO_2. Work was conducted in a laminar flow bench.

4.1.2 Passaging

Cells were passaged when reaching 90% confluency. Media was removed, the cells were then washed once with PBS pH 7.4. Then trypsinized with 1 ml 0.25% Trypsin for 10 cm plate (2 ml for 15 cm plate) in an incubator (37℃ with 5% CO_2) for approx 5 min until cells were lifted off by tapping the plate. 10 ml 37℃ DMEM was then added, and cells were resuspended and split to new plates.

4.1.3 Freezing

Cells were trypsinized as under 4.1.2. Suspended cells were centrifuged for 4 min at 900 rpm, then resuspended in 90% complete DMEM, and 10% Dimethyl Sulfoxide (DMSO). Cells were put in a CryoPure freezing tube, stored at −20℃ for 1 h before moving to −80℃ for max one week before being moved to liquid nitrogen.

4.1.4 Thawing

Cells were thawed completely in a 37℃ water bath after retrieval from liquid nitrogen. 6 ml 37℃ complete DMEM was added before centrifugation for 5 min at 900 rpm. Cells were resuspended in 10 ml 37℃ complete DMEM, then plated, and incubated as under 4.1.1.

4.1.5 Transfection

Foreign DNA was introduced into eukaryotic cells using Lipofectamine 3000 (Table 3.7). Lipofectamine works by forming liposomes, entrapping DNA, and allowing the DNA to enter cell membranes.

The cells were grown to approximately 80% confluency in appropriate sized dishes (6-well or 10 cm plates) (if for immunostaining they contained two coverslips). The medium was before transfection changed to P/S free DMEM; the cells were kept at 37℃ until the transfection solution was added. Lipofectamine 3000, and P3000 were diluted in Opti-MEM® Reduced-Serum Medium (Opti-MEM) according to Table 4.1. The plasmid was then added to P3000 dilute, and mixed. The P3000/DNA dilute was then added to each their own lipofectamine dilute, and incubated for 15 minutes at RT to let the DNA-lipofectamine complexes to form.

Table 4.1: **Reagents used during transfection.**

Dish size	6-well	10 cm
Opti-MEM	125 µl	250 µl
P3000	4 µl	20 µl
Plasmid	2 µg	10 µg
Lipofectamine 3000	3 µl	24 µl

Each mix was then added dropwise to an appropriate dish. The cells were then left to incubate for 24-48 h. After incubation they were either fixated and then immunolabeled as under section 4.1.6) or a whole cell extract was prepared as in section 4.1.7.

4.1.6 Immunolabelling

Cells were plated on coverslips placed in 6-well plates. The transfection was then carried out as in section 4.1.5. Cells were then fixed with 3.7% paraformaldehyde (PFA) in PBS for 10 min 24-48 hours after transfection. PFA was then removed, and the slips were then washed 3× with PBS. Cells were then permeabilised by incubation with 0.25% Triton-X100 in PBS for 10 min.

After permeabilization cells were blocked by incubating with 60 µL blocking buffer (5-10% Goat Serum diluted in 0.1% 2-[4-(2,4,4-trimethylpentan-2-yl)phenoxy]ethanol

(Triton-X100)/PBS) for 1 h. The slips were then incubated with primary antibody diluted (Table 3.2) in blocking buffer for 1 h at RT. They were then washed 4×5 min with PBS, before incubating with secondary antibody diluted (Table 3.2) in blocking buffer for 1h at RT.

Slips were then washed three times with PBS for 5 min. The slips were dipped in fresh Milli Q, drained, and then mounted on freshly cleaned glass coverslips with ProLong™ Glass Antifade Mountant with NucBlue™ Stain (NucBlue mounting medium). Slips were incubated at RT for 10 min, before being put in storage (4℃, dark).

Subsequent imaging was conducted using a Leica DMI6000 B microscope (Table 3.5).

4.1.7 Whole cell extraction

80% confluent cells grown on 10 cm plates were washed with PBS, before scraping with 0.5 ml radioimmunoprecipitation assay buffer (150 mM NaCl, 50 mM Tris, 5 mM EDTA, 1.0% nonylphenylpolyethylene glycol (Igepal), 0.5% Sodium deoxycholate, 0.1% sodium dodecyl sulfate (SDS)) (RIPA). The cells were then collected and incubated on ice for 15 min. The lysate was then sonicated 3×5 sec in 1 min intervals, before centrifuging for 5 min at 13000× g, and 4℃. The supernatant was collected as whole cell extracted, and stored at −80℃.

4.1.8 Cytoplasmic, and nuclear fractionation

All steps during the fractionation were done on ice, using ice-cold buffers, tubes, and syringes used. Cells were grown in a 15 cm dish to approximately 80% confluency, then washed 2× with PBS. The cells were then washed briefly with 10 mM Tris pH 7.8, in order to remove salt from PBS. Before being scraped with hypotonic buffer (10 mM tris(hydroxymethyl)aminomethane (Tris) pH 7.8, 1.0% Igepal, 1 mM dithiothreitol (DTT), 1:100 mammalian protease inhibitor cocktail, and 2 mM Na_3VO_4). The cells were collected and incubated on ice for 3 min. Equal volume ddH_2O was added to the lysate, before incubating for another 3 min. Cells were then sheared 8× through a 23-gauge syringe, before being centrifuged at 1 000× g at 4℃ for 6 min. The supernatant containing the cytoplasmic fraction was centrifuged an additional time at 1 000× g at 4℃ for 6 min to remove nuclear contamination. The supernatant was then stored at -80℃.

The nuclear pellet was re-suspended in 1 ml Washing buffer (10 mM Tris pH 7.5, and 2

mM $MgCl_2$). Resuspended pellets from RL95-2 cells were sheared again 8× through a 23-gauge syringe to remove cytoplasmic components left. The fraction was centrifuged at 1 000× g at 4℃ for 6 min. The supernatant was removed, and the pellet was resuspended using 100 µl RIPA (50 mM Tris pH 8.0, 0.5% deoxycholic acid, 150 mM NaCl, 1.0% Igepal, 0.1% SDS, 2 mM Na_3VO_4, and 1× Protease Inhibitor Cocktail) . The nuclear fraction was then vortexed for 1 min, at full speed, then sonicated in a sonication bath for 2 min. The fraction was then centrifuged one last time at 16'200× g, at 4℃ for 6 min. The supernatant was collected as a nuclear fraction, and stored at -80℃.

4.2 PCR techniques

Polymerase chain reaction (PCR) is a flexible and well-established method. Its primary use is to make large copy number of short DNA sequences. PCR was used for varying uses in this thesis: reverse-transcription polymerase chain reaction (RT-PCR), cloning, site directed mutagenesis (SDM), and sequencing.

4.2.1 RT-PCR

RT-PCR is a PCR technique that, among other uses, allows one to detect RNA present within the cell. It works by first reverse transcribing RNA into complementary DNA (cDNA). Both RNA extraction and cDNA synthesis was already conducted by another lab member (Appendix: 6.5, 6.6).

The cDNA sample was used in a PCR together with one of the forward primers targeting the Q68 insert "Forward Insert 7591/7495/8001", and the reverse primer "Reverse sequencing primer" (see table 3.6). This PCR was run using the Phusion High-Fidelity kit (Table 3.7). Each PCR was run in 50 µl volume with 100 ng cDNA template, 0.1 µM Forward primer, 0.1 µM Reverse primer, 1 mM $MgCl_2$, 2.5% DMSO, 0.2 mM dNTP, HF buffer (1.5 mM $MgCl_2$), and 2.0 U Phusion (polymerase). The PCR was then run, as stated in table 4.2. A sample of each PCR reaction conducted was subsequently run through a 1% agarose gel as in section 4.5.

Table 4.2: **Thermal program for RT-PCR.**

	Temperature (℃)	Time (mm:ss)	Cycles
1st Denature	98	5:00	
Denature	98	0:10	
Anneal	48	0:30	×42
Extension	72	0:10	
Last extension	72	7:00	
Hold	10	∞	

In order to sequence the PCR product, any visible bands of approximately correct resolving pattern were extracted as described in section 4.5.1.

4.2.2 Cloning

The restriction sites Eco-RI, and XhoI; and the Kozak sequence present in WT p110β was added to an open reading frame (ORF) p110β, using the Forward EcoRI pcDNA 110β, and Reverse EcoRI pcDNA p110β(Table 3.8). The PCR was run with 1.0 ng DNA template, 0.1 µM Forward primer, 0.1 µM Reverse primer, 1 mM $MgCl_2$, 2.5% DMSO, 0.2 mM dNTP, 1× HF buffer (1.5 mM $MgCl_2$), and 2.0 U Phusion (polymerase). The PCR was then conducted as in table 4.3.

An ORF sequence corresponding to the Q68 was cloned into a pEGFP-C1 vector, to generate the Q68-EGFP fusion protein tagged at the N-terminus. The PCR was carried out as above, but with the forward XhoI Q68, and reverse EcoRI Q68 primers instead.

Table 4.3: **Thermal program for cloning PCR.**

	Temperature (℃)	Time (mm:ss)	Cycles
1st Denature	98	2:00	
Denature	98	0:10	
Anneal	55	0:30	×35
Extension	72	2:00	
Last extension	72	7:00	
Hold	10	∞	

The cloning PCR product was then purified by column purification, using the NucleoSpin®

Gel and PCR Clean-up kit (Table 3.7), then fused to a vector digested with the EcoRI, and XhoI restriction enzymes. The digestion was conducted by incubating 5 µg plasmid (pcDNA 3.1(+) for the "Kozak" cloning, and pEGFP-C1 for the Q68 cloning), CutSmart, 40 U XhoI, and 40 U EcoRI, for 1.5 h at 37℃.

A fusion of the vector and purified PCR product was then conducted by mixing 80 ng vector, 60 ng purified PCR product, and 0.2 (v/v) Fusion Enzyme mix; and incubating for 15 min at 50℃. The fusion product was then transformed as in section 4.3.

4.2.3 Site-Directed mutagenesis

SDM was used to introduce mutations to DNA. Two SDM's were conducted during this thesis; the introduction of restriction sites, and a Kozak sequence to the start of a p110β sequence with primers "Forward EcoRI pcDNA p110β", and "Reverse EcoRI pcDNA p110β"; and the introduction of the 15 bp insert predicted to be part of Q68 by the "Forward Q68 Insert", and "Reverse Q68 Insert" (Table 3.8). The PCR solution contained 10 ng plasmid template, 0.2 µM forward, and reverse primer (Table 3.6), 2.5% DMSO, 2.5 mM $MgCl_2$, 2.5 mM dNTP, HF buffer, and 2 U polymerase (Phusion). The PCR was then conducted as in table 4.4.

Table 4.4: **Thermal program for SDM PCR.**

	Temperature (℃)	Time (mm:ss)	Cycles
1st Denature	95	0:30	
Denature	95	0:30	
Anneal	Tm	1:00	×25
Extension	68	1:00 pr kBp	
Last extension	68	7:00	
Hold	10	∞	

10-20 U of DpnI was added to the PCR product, and incubated for 1 h, at 37℃) in order to digest methylated DNA, i.e. non-PCR product. The digested product was then transformed as in section 4.3.

4.2.4 Sequencing

DNA samples were sequenced using the BigDye v.3.1 protocol. PCR was conducted with DNA sample as shown in table 4.6, with 0.1 (v/v) Big Dye solution, 0.1 (v/v) Sequencing buffer, and 0.01 (v/v) sequencing primer (Table 3.6), and run as described in table 4.5. Samples were then delivered to the sequencing facility to be sequenced.

Table 4.5: **Thermal program for sequencing PCR.**

	Temperature (℃)	Time (mm:ss)	Cycles
1st Denature	98	5:00	
Denature	98	0:10	
Anneal	55	0:05	×30
Extension	60	4:00	
Hold	10	∞	

Table 4.6: **Amount (ng) of DNA template used during sequencing PCR.**

PCR product length (bp)	Mass (ng)
100-200	1-3
200-500	3-10
500-1000	5-20
1000-2000	10-40
>2000	20-50
Single-stranded	25-50
Double-stranded	150-300

4.3 Transformation

Transformation was done in order to create a large copy number of target DNA sequence. 2.7 µl DNA was added to 50 µl cells and mixed by pipetting once. The cells were then incubated on ice for 30 min, followed by heat-shock at 42℃ for 45 seconds. The cells were then immediately transferred to ice and incubated for 2 min. Cells were subsequently incubated for 1 h at 37℃, and 250 rpm after adding 80 µl Super Optimal Broth (SOC) medium (Table 3.1.2). The cells were then plated to an appropriate antibiotic containing 10 cm agar plate and incubated upside down overnight, at 37℃. The plates were stored at 4℃.

4.4 Inoculation

Four colonies were picked from the agar plate and grown in 5 ml LB-medium (Table 3.1.2) with appropriate antibiotics at 37℃ at 250 rpm overnight. The samples were then centrifuged at 5 200 ×g for 15 min at 4℃. The pellet was then collected, and Mini-prep was conducted as described in the "Nucleospin® Plasmid/Plasmid No Lid" protocol.

4.5 Agarose gel electrophoresis

Agarose gel electrophoresis was used to separate DNA fragments based on their size. 1–2% agarose was added to Tris-acetate-EDTA (40mM Tris, 20mM Acetate, and 1mM Ethylenediaminetetraacetic acid (EDTA)) (TAE Buffer), and brought into solution by boiling. 0.5 µg/ml ethidium bromide (EtBr) was added and mixed. The gel was then cast at room temperature in a gel casting kit with a comb. The electrophoresis was run in a gel electrophoresis block with the gel submerged in TAE Buffer, at 100V. The gel was then imaged using a Gel Doc™ EZ (Table 3.5).

4.5.1 Agarose gel extraction

DNA Bands from agarose gels were extracted and purified following the protocol by Macherey-Nagel with their NucleoSpin® Gel and PCR Clean-up (5.2) protocol (Table: 3.7).

4.6 Protein concentration determination

The concentration of protein solutions were determined by bicinchoninic acid assay (BCA). 4 µl protein sample and 4 µl of BCA standard mix (0.0, 0.5, 1.25, 2.5, 5.0 µg/ml) were pipetted in triplicate to a 96 well plate. Bovine serum albumin (BSA) and protein were diluted in the same buffer. 200 µl of BCA Protein Assay Reagent mix (50:1 Pierce™ BCA Protein Assay Reagent A, Pierce™ BCA Protein Assay Reagent B) was then pipetted onto each of the loaded wells, then incubated for 10 min at 37 ℃. The absorbance was subsequently read at 562 nm with an Epoch™ Microplate Spectrophotometer.

4.7 SDS-PAGE

Protein samples were separated based on molecular weight by using sodium dodecyl sulfate-polyacrylamide gel electrophoresis (SDS-PAGE). A protein is denatured, given a negative charge, and subjected to an electrical field. The applied field migrates proteins towards the positive anode at different rates, where smaller proteins migrate faster than larger proteins.

SDS gels were made with 10% acrylamide/bisacrylamide (37.5:1) at 1.5 mm thickness (Table 3.1.3). Protein samples were mixed with Laemli sample buffer (Table 3.1.3). Samples were boiled at 100 ℃ for 5 min and kept on ice until loaded into the gel. Electrophoresis was conducted at 100 V. The gel was then used for western immunoblotting.

4.8 Western immunoblotting

Proteins were visualised by transferring them from an SDS gel onto a nitrocellulose membrane at 200 V for 2h in ice, or at 20-50 V O/N at 4 ℃ in transfer buffer (Table 3.1.3). The membrane was washed 4×5 min with TBS-T (Table 3.1.3) afterwards, then blocked with 7% Milk in TBS-T for 1h on a shaker. Diluted milk was washed away by 2x rinses using TBS-T, before adding the primary antibody (Table 3.2), and incubating for 2 h on a shaker at RT or O/N on a shaker at 4℃. Afterwards, blots were washed 4×5 min using TBS-T on a shaker, and the secondary antibody was then added (Table 3.2) and incubated for 1 h at RT on a shaker. Blots were then again washed 4×5 min with TBS-T. Blots were visualised by first treating them with enhanced chemiluminescent (ECL) of either Pico or Femto variant (Table 3.7), depending on band strength. A Bio-Rad CheiDoc™ XRS+ System (Table 3.5) was used for imaging.

After visualising the primary probe, the loading quality was then assessed. First, the blots were stripped by incubating them with stripping buffer for 7 min at 37℃. The blots were then blocked again with 7% milk in TBS-T for 1h on a shaker. Diluted milk was washed away by 2x rinses using TBS-T, before adding lamin A/C (Table 3.2), and incubating for 2 h on a shaker at RT or O/N on a shaker at 4℃. Afterwards, blots were washed 4×5 min using TBS-T on a shaker, and the secondary antibody was then added (Table 3.2) and incubated for 1 h at RT on a shaker. Blots were then again washed 4×5 min with TBS-T, and imaged, as above. The blot was then stripped, blocked, incubated with the primary antibody α-tubulin (Table 3.2), washed, and imaged as above.

If visualisation with these antibodies did not work, ponceau (0.1% (w/v) in 5% acetic acid,

0.5 g ponceau S, 250 ml acetic acid) was used, instead. Blots were washed 2× with TBS-T, before adding ponceau and incubating for 30 min on a shaker at RT. Afterwards, blots were washed 4×5 min using TBS-T on a shaker and imaged.

5 Results

p110β has been detected in not only the cytoplasm but also in the nucleus of non-transformed cell lines (Kumar et al. 2011). Our group has also detected p110β in both cytoplasmic, and nuclear fractions from several endometrial cancer cell lines, including RL95-2, and MFE-319 (Gavgani, Karlsson, et al. 2019). Our laboratory has tested for p110β localisation using two different antibodies, one N-terminal (Santa Cruz, from AA 2-31) (Gavgani, Karlsson, et al. 2019), the other more C-terminal (Abcam, from AA 400-500) (unpublished data). These antibodies showed different resolving patterns, with the C-terminus antibody showing additional lower bands. We attempted to validate these findings by using a different set of antibodies, the same Santa Cruz, and a more C-terminal antibody (Thermo Fisher, AA: 411-605).

5.1 Two antibodies against p110β show dissimilar resolving pattern

We decided to probe whole, cytoplasmic, and nuclear fractions with two different anti-p110β antibodies, one from Santa Cruz, and the other from Thermo Fisher (Table: 3.2), that recognises the area in p110β as shown in figure 5.1, in order to observe the different resolving pattern. Fractions were obtained as discussed under section 4.1.7 and 4.1.8, then resolved by SDS-PAGE, before they were probed using the two different antibodies against p110β (Figure 5.1 A, and B).

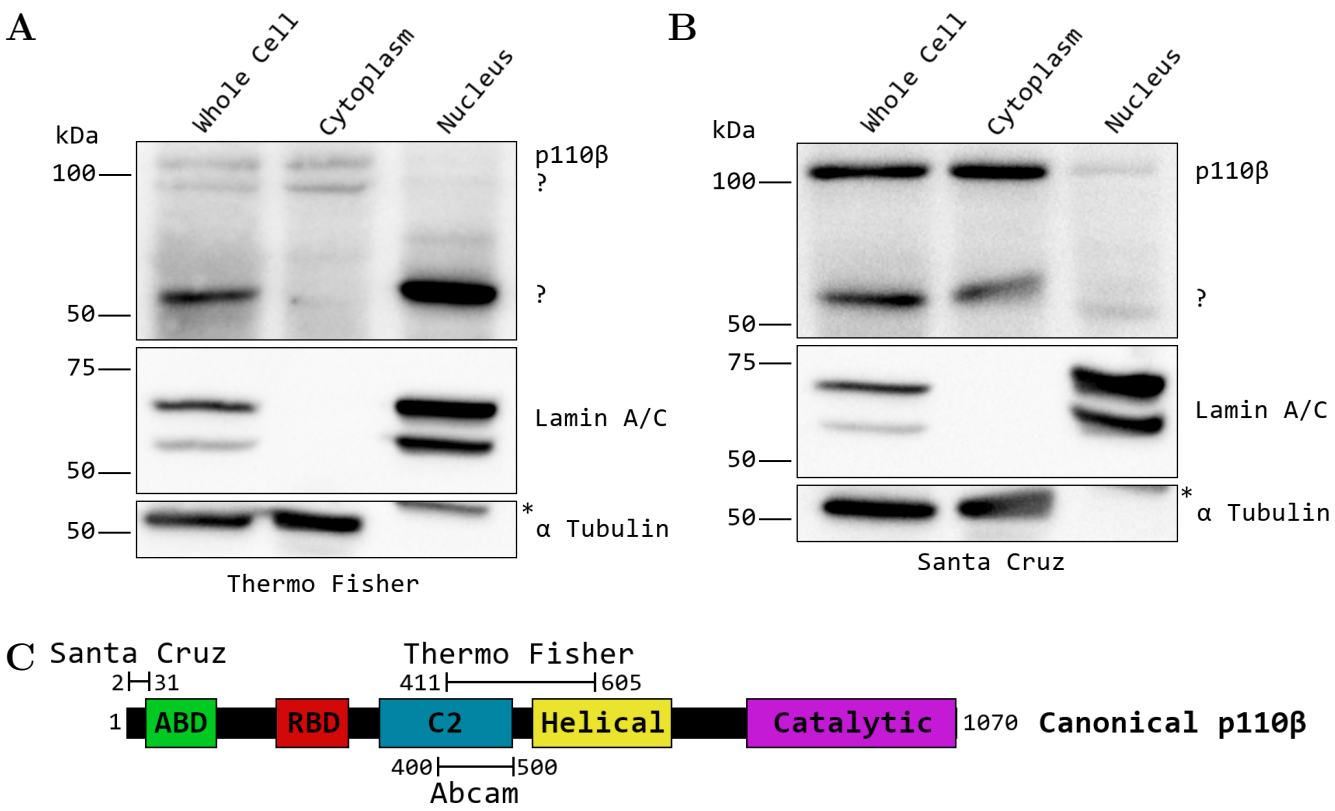

Figure 5.1: **RL95-2 cell fractions probed with p110β antibodies showing the differing resolving pattern.** Proteins obtained from whole (100 µg), cytoplasmic (50 µg), and nuclear extract (30 µg) from RL95-2 were resolved with SDS-PAGE, then transferred onto a nitrocellulose membrane. *The band above α-tubulin in the nuclear fractions are from residual lamin A/C staining that was not stripped completely. **A)** One membrane was then western blotted with Thermo Fisher anti-p110β (#703364). Lamin A/C and α-tubulin were then used to verify loading purity for nuclear and cytosolic fraction, respectively. **B)** Another membrane was western blotted with a Santa Cruz anti-p110β (#376641). Lamin A/C and α-tubulin were then used to verify loading purity for nuclear and cytosolic fraction, respectively. **C)** Depicted model of the canonical p110β form. Binding sites in regards to amino acid number, and location for the epitopes of the Santa Cruz, Thermo Fisher, and Abcam antibodies are shown. Abbreviations: ABD - Adaptor Binding Domain, RBD - Ras Binding Domain.

100 µg whole cell extract, 50 µg, cytosolic, and 30 µg nuclear fraction were loaded in order to compensate for varying concentrations of p110β within each fraction.

The Thermo Fisher antibody binds to amino acids number 411 until 605 (*PIK3CB Antibody (703364)* 2020), as seen in figure 5.1 C), and showed two bands around the 100 kDa marker; one above, one underneath, in both whole, and cytosolic fractions. Our group have observed this pattern before; the band above 100 kDa marker has always been present when probing with anti p110β antibodies and is consistent with the canonical form of p110β. The lower band has only been observed for some antibodies, in some cell lines

(Gavgani, Karlsson, et al. 2019, and Kumar et al. 2011)). What this lower band indicates is so far unknown. Meanwhile, a stronger band resolved above the 50 kDa marker in both the whole and nuclear fraction (Figure 5.1 A).

The antibody supplied by Santa Cruz binds to amino acids number 2 until 31 (*PI 3-kinase p110β Antibody (C-8)* 2020) (Figure 5.1 C). Probing with this antibody showed a band above 100 in all of the samples, but a weaker band in the nuclear fraction. The antibody also detected bands above 50 kDa in both the whole and cytosolic fractions. There were also a detectable band at the same resolving height in the nuclear fraction, albeit much weaker (Figure 5.1 B). The bands at around 50 kDa migrated lower for the Thermo Fisher antibody compared to Santa Cruz. This matches an observation made earlier by our group when probing with both of these antibodies on the same blot (non-published data).

The purity of each fraction was confirmed by probing with antibodies against proteins that are located in distinct fractions, and are ubiquitously expressed. Lamin A/C is located within the nuclear lamina (Gerace, Blum, and Blobel 1978), and antibodies against Lamin A/C will therefore only stain fractions containing this nuclear protein. Figure 5.1 show Lamin in both whole, and nuclear, but no bands in cytosolic fraction for both antibody-blots. An antibody against α-Tubulin, a 50 kDa mass protein was used to show purity in regards to cytoplasmic fraction, as it is not found within the nucleus. Figure 5.1 show α-tubulin in both whole, and cytoplasmic fractions.

5.2 The predicted Q68 isoform is expressed in RL95-2 cells

The results shown in figure 5.1 suggests the possible presence of a p110β isoform with a mass of about 50 kDa. Candidates that would fit the lower p110β band in figure 5.1 was searched for on Ensemble. At the time of writing there were five sequences predicted to produce novel proteins, listed as "protein coding biotypes" [1]. Out of these, two entries were seen as possible candidates for the observed lower band in figure 5.1 A). The most likely candidate was a sequence with UniProt code "Q68DL0" (*PIK3CB - Phosphatidylinositol 4,5-bisphosphate 3-kinase catalytic subunit beta isoform - Homo sapiens (Human) - PIK3CB gene & protein* 2020) henceforth referred to as "Q68". Q68 had a predicted mass of 59,770 Da. It was also the only sequence (besides the canonical form) with a transcript support level (TSL) Category one 1 (Appendix, figure 6.1). The other candidate: H0Y871 was deemed a less plausible candidate because of its lower TSL score of 2, its mass was also more dissimilar to the resolved bands in figure 5.1 A), at a theoretical mass of 80.5 kDa.

[1] Defined on ensambl as: Gene/transcipt that contains an open reading frame (ORF).

TSL is calculated by comparing mRNA, and expressed sequence tag (EST) alignments to GENCODE transcripts. For sequences with a TSL category of 1: "all splice junctions of the transcript are supported by at least one non-suspect mRNA" [2] (*Transcript flags* 2020, and *Gene: PIK3CB - Ensembl* 2020).

Q68 was predicted to start at the ATG codon from base pair 1663-1665, located inside the helical domain of canonical p110β. Both the canonical and the predicted shortform share the same stop codon. Q68 was predicted to contain an insertion of 15 bases compared to the canonical p110β inside the catalytic domain. This insert is identical to 15 base pairs of the intron upstream of canonical exon 17 (Figure 5.2 A) . Three primers (7495, 7591, and 8001; Table 3.6) were designed to align to the Q68 insert (Figure 5.2 B), to test for the possible isoform's presence at the mRNA level and then used in an RT-PCR against RL95-2 RNA extract.

To test for the possible isoform's presence at the mRNA level, three primers (7495, 7591, and 8001; were designed to align to this insert as seen in figure), and used in a RT-PCR against RL95-2 RNA extract.

[2]Suspect mRNA is defined by Ensembl as "Erroneous transcripts and libraries identified in lists maintained by the Ensembl, UCSC, HAVANA and RefSeq groups are flagged as suspect."

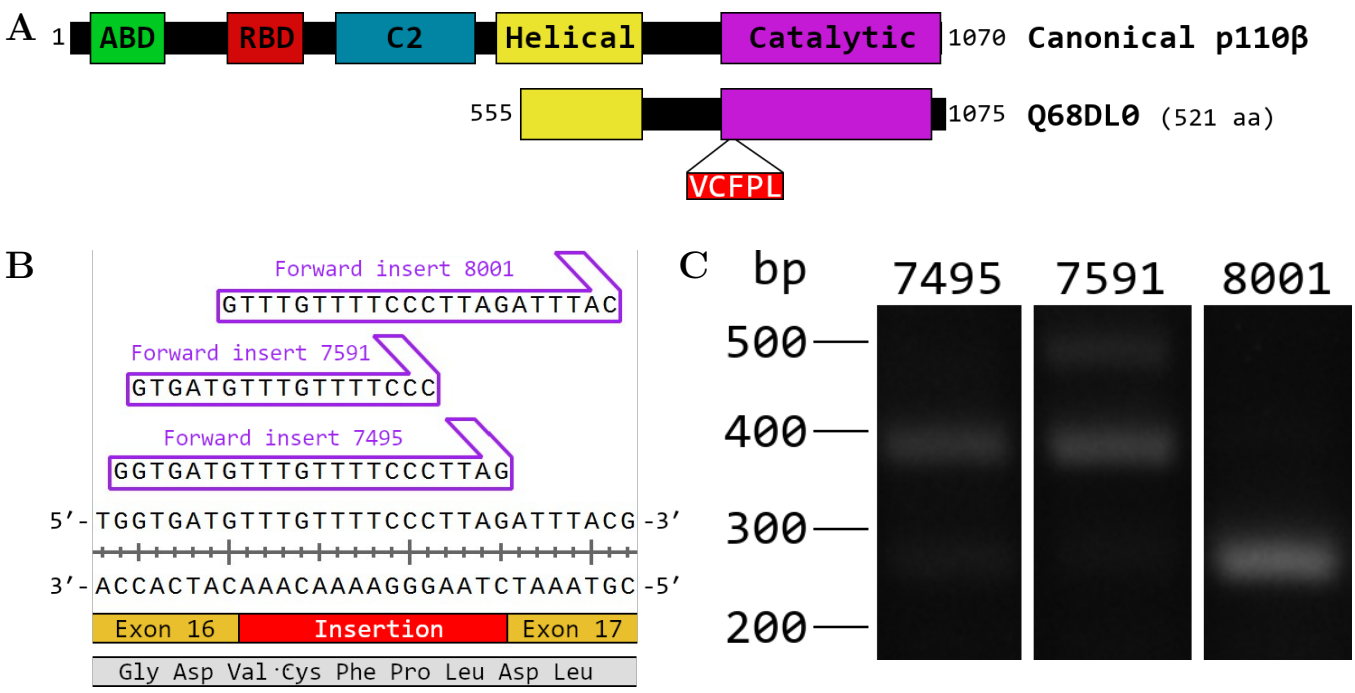

Figure 5.2: **RT-PCR on predicted Q68 insert produced DNA band of predicted length. A)** Model of both the canonical p110β and the predicted shortform Q68 (Q68DL0). Amino acid changes from the predicted insert of Q68 highlighted in red (DDL → DVCFPLDL). **B)** Forward primers designed against the Q68 insertion, located within the canonical intron 17. Three primers were designed to amplify the DNA sequence, including the insert found in the predicted Q68 inform from cDNA. The insert sequence is marked in red. **C)** 1% agarose gel of PCR product of cDNA with three forward primers (7495, 7591, and 8001) targeting the Q68 insert, and the reverse sequencing primer (Table 3.8). The PCR products were then run through a 1% agarose gel to separate the PCR products based on size, using ethidium bromide for staining. The resulting gel was then imaged using a Gel Doc™ EZ.

The resulting PCR products were separated by use of agarose electrophoresis (Figure 5.2 C)). Although the successful PCR should resolve one band at about 250 bp, both primer 7495, and 7591 unexpectedly resolved into two bands correlating at 400 bp, with 7592, resolving an additional band at 500 bp. Meanwhile, primer 8001 had one band, correlating in between the 300, and 200 bp marker. All of the bands were extracted and then sequenced, as PCR of the insert had proven difficult.

Sequencing of the 400 bp, PCR products obtained from the " 7495" primer, and the 500 bp "7591" primer gave sequences that aligned with "Pan paniscus DEAD-box helicase 3 X-linked (DDX3X), transcript variant X3, mRNA", using blast. The 400 bp band for the "7591" primer gave no sequence product. Of note, none of the primers, when blasted with Primer-Blast from the national center of biotechnology information (NHI) during primer design, aligned to the "Pan paniscus DEAD-box". The band from primer "8001" gave a

sequence aligning to Q68's theoretical sequence, including its insert, and 200 bp downstream, as seen in figure 5.3.

The sequence obtained from the PCR product using primer 8001, aligned with the predicted insert, and downstream bases of the Q68 isoform, as seen in figure 5.3. The alignment between the Q68 theoretical sequence and sequence result from primer 8001 is shown in figure 5.3 A. The insert is highlighted red, with the sequencing histogram over the insert area shown in figure 5.3 B). In summary, the RL95-2 cells are likely to express the predicted Q68 isoform at the mRNA level.

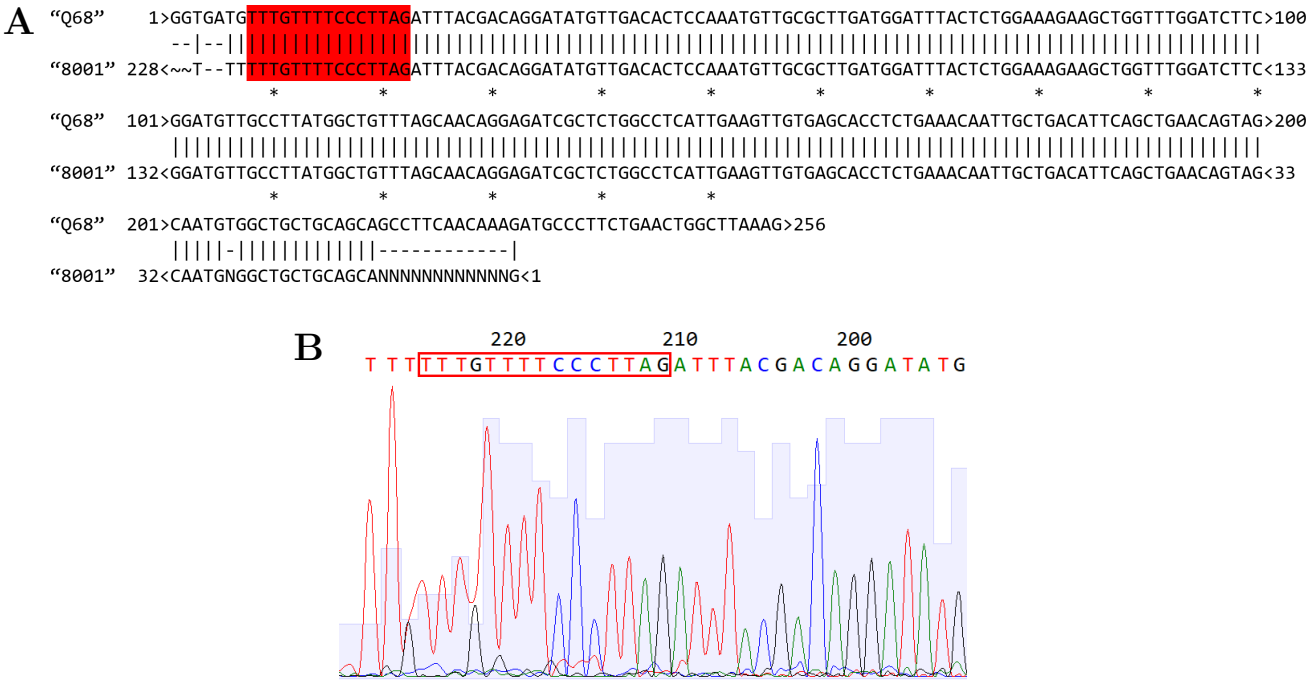

Figure 5.3: **RL95-2 cell expressed the Q68 isoform. A)** The cDNA obtained from RL95-2 cells was used in RT-PCR with a primer targeting the insert within Q68. The reverse primer was located about 200 bp downstream. The PCR product was subsequently sequenced, using the same reverse primer. The alignment between the theoretical Q68 DNA sequence ("Q68"), and the PCR product sequence ("8001") is depicted in 5′ to 3′ direction. Matches between each sequence are denoted by a (|), and mismatches are denoted by (-). **B)** The histogram obtained by sequencing, shows the area covering the insert, and downstream sequence. Each base pair's relative signal strength is denoted by the height along the y-axis of each coloured line. Adenine (A) is denoted by green, thymine (T) by red, cytosine (C) by blue, and guanine (G) by black.

5.3 p110β and Q68 have different Kozak sequence strengths.

In order to further test the transnational ability of Q68, we needed to construct further experiments; during this, the *PIK3CB* gene was analysed.

A possible Kozak sequence was found during the analysis for the possible isoform Q68. Kozak sequences are conserved sequences surrounding the start codon (AUG) in mRNA and facilitate translation. While a Kozak sequence is not necessary for translation, stronger Kozak sequences are often tied to higher expression of genes. The most typical Kozak sequence is: CC$\underline{\text{A}}_{\underline{\text{G}}}$CC**ATG**$\underline{\text{G}}$GC, with the underlined bases being the most conserved (Kozak 1989). Both the canonical p110β and Q68 isoforms contain a Kozak sequence, with the canonical being; TTATGA**ATG**TG; and Q68 isoform being: AATGAA**ATG**GA. The canonical form p110β only contain secondary Kozak sequence bases. The Q68 contains the two most conserved bases, -3, G; and +1, G. Thus the Q68 may contain a stronger Kozak sequence, leading possible independent translation.

5.4 HeLa cells express low levels of canonical p110β

In order to test the transnational ability of Q68, we constructed two experiments; the first would mutate the ATG's of the p110β isoforms, and observe the transnational differences between the mutants. The other experiment was an overexpression quantification experiment. In order to conduct theses experiments, we would needed a model cell line containing low levels of expressed p110β, and the possible Q68 isoform. So that most of the expressed p110β and Q68 would be from the transfection.

The levels of p110β was tested for in the cell lines HEK, and HeLa; These cell lines have already observed to naturally express lower levels of p110β when compared to RL95-2 cells by our lab. We extracted whole cell extract from HEK and HeLa cells as in section 4.1.7. 70 µg of each fraction were separated based on size using SDS-PAGE, then transferred to a nitrocellulose membrane to probe with the Thermo Fisher anti-p110β antibody. The α-tubulin antibody was used as a marker for equal loading between the wells.

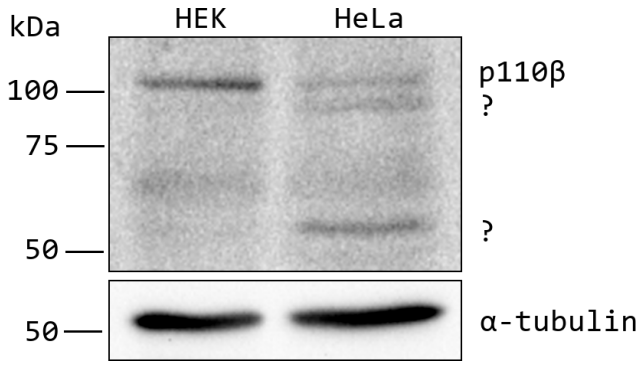

Figure 5.4: **p110β levels in, HEK, and HeLa cell lines, observed by western immunoblotting with anti-p110β of whole cell extract.** The proteins (70 µg) obtained from whole cell extract from HEK or HeLa cells were resolved with SDS-PAGE, and then transferred onto a nitrocellulose membrane. The membrane was then probed with a Thermo Fisher anti-p110β antibody. α- tubulin, was then used to verify equal loading (Table 3.2).

Each of the cell line extracts showed a band correlating above the 100 kDa marker consistent with the canonical isoform. The HeLa cells fraction contained an additional band, correlating bellow the 100 kDa marker. This is consistent with previous blots made by our group using HeLa, and the Thermo Fisher antibody. Another band correlated above the 50 kDa marker. This band may correspond to the Q68 isoform, but it is also possible to be a degradation product of canonical p110β.

We chose to use HeLa for our experiments, as they proved more amenable during transfection, even though neither of these lines were optimal, in regards to p110β vs Q68 levels.

5.5 Mutation of ATG of short isoform Q68 may halt its translation

A proof for the existence of the Q68 isoform would be to show that the resolving pattern would change based on isoform knockout. If we were to knock out the canonical p110β, one would expect no band above 100 kDa, while keeping the band above 50 kDa when staining with the Thermo Fisher antip110β antibody. Inversely, knockout of Q68's ATG should result in the opposite effect.

A WT of p110β missing the pre-ATG Kozak sequence had its Kozak sequence re-introduced, (section 4.2.2), using the primers "Forward / Reverse EcoRI pcDNA p110β" (Table 3.6). This was then fused into a pcDNA 3.1(+) vector (Table 3.8) (Section 4.2.2).

Two mutants were created from this vector, each with either the canonical p110β's or Q68's start-codon mutated to AAC. This was done by SDM using either the "Forward / Reverse 1st ATG knockout", or with "Forward / Reverse 2nd ATG knockout" primers (Table 3.6). The success of each of these mutations was confirmed by sequencing.

HeLa cells were then subjected to transfection using either the WT ATG p110β (WT ATG p110β), Kozak p110β with the canonical ATG mutated (1st ATG mutant), or with Kozak p110β with the Q68's ATG mutated (2nd ATG mutant) as described in section 4.1.5. A control group was also run with no plasmid added during transfection. After 24 h transfection whole cell extract was collected, and proteins were resolved by SDS-PAGE and transferred to a nitrocellulose membrane for probing. The loading quality was confirmed with ponceau. While lamin A/C or α tubulin would have been preferable control probes, as these give a specific signal to either the nucleus or the cytoplasm, imaging of these did not work.

All of the samples contained a band above the 100 kDa marker, with the WT p110β sample's 100 kDa band being slightly higher. The transfected samples contain a band correlating underneath the 75 kDa marker, with the cell extract obtained from transfection with "Kozak p110β 2nd" primer having a stronger band. Sample 1,3, and 4 contained a band above the 50 kDa marker, possibly corresponding to the Q68 isoform.

The blot points to the fact that our transfection was not entirely successful, as the band strengths are similar for all wells, when one would expect the control to have a weaker signal. Besides, while we do observe a reduction in the canonical signal in the 1st ATG mutant sample, we see no reduction of signal in the Q68 appropriate band in the 2nd ATG mutant sample.

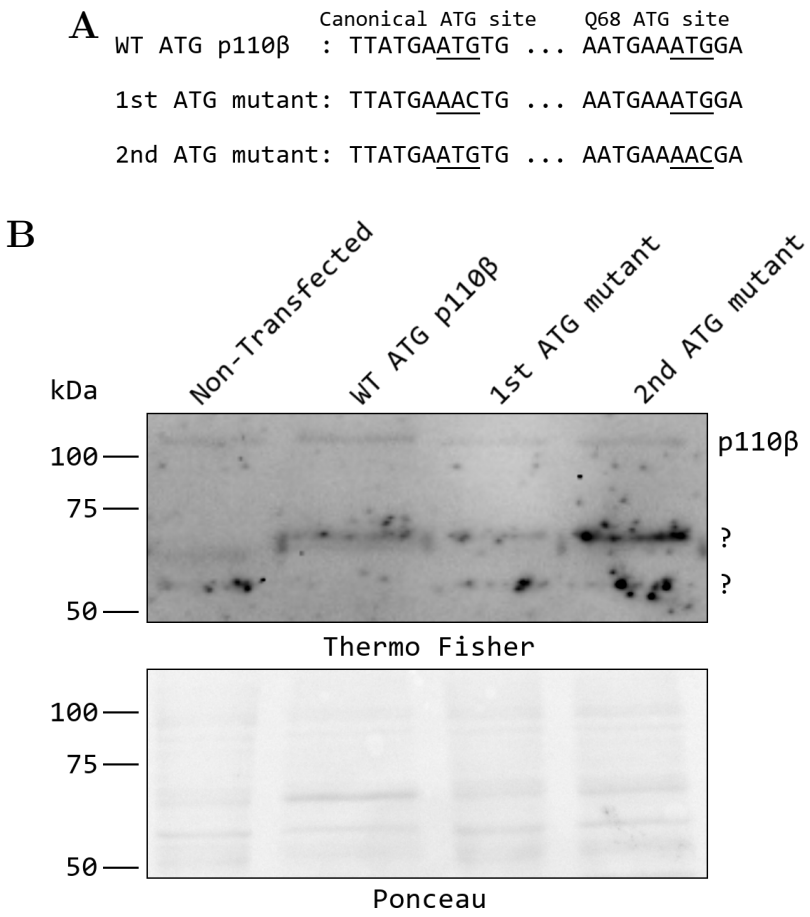

Figure 5.5: **p110β translation levels visualized by western blot, using Thermo Fisher anti-p110β. A)** Diagram of the Kozak of the three different constructs. **B)** HeLa cells were transfected with three p110β mutants: p110β containing its Kozak sequence, canonical ATG mutated to AAC, or Q68 ATG mutated to AAC. Proteins were then obtained by whole cell extract and separated based on size with SDS-PAGE. 23.1 µg protein was loaded, then transferred onto a nitrocellulose membrane. The membrane was then probed with a Thermo Fisher anti-p110β. Ponceau was used to verify the loading volume equality.

5.6 Quantification of expressed phenotypes for p110β, and its possible shortform Q68, when overexpressed.

With western blots hinting at a possible nuclear localisation of Q68 (Figure 5.1) we wanted to determine, and quantify the localisation of the Q68 isoform within the cell, in comparison to the canonical p110β form.

An open reading frame (ORF) sequence of p110β and Q68 were cloned into pEGFP-C2-, and pEGFO-C1 vectors as in section 4.2.2, to generate the fusion protein with the tag in

the N-terminus [3]. The transfections were conducted on HeLa cells grown in 6-well plates, as described under section 4.1.5. A control group was also run each time in parallel, were HeLa cells were transfected with an empty EGFP construct. The cells were then fixated and imaged as described under 4.1.6 before being counted manually.

In total, five patterns were observed, with the pattern of nuclear preference being exclusive to the control group. The observed patterns during cell counting were "continuous", "nuclear preference", "cytoplasmic preference", "small vacuoles", and "large vacuoles". Cells showing an even distribution of EGFP signal over the entire cell was labelled as having a continuous pattern. Cells, where the EGFP signal was stronger within the nucleus were counted as having a "nuclear preference". In contrast, cells that had a stronger signal in the cytoplasm were counted as "cytoplasmic preference". A subset of cells with cytoplasmic preference contained what appeared to be small vacuoles; these were counted as having a "small vacuoles" pattern. Lastly, a small number of cells contained EGFP signal in larger vacuoles; these were counted as having the "large vacuoles" pattern. Examples for each of these patterns are shown in figure (Fig 5.6).

[3]Different vectors were used because the pEGFP-C2-p110β was already made before this thesis began. When we then created the EGFP-Q68 we were out of pEGFP-C2 vector, the discrepancy was judged as tolerable.

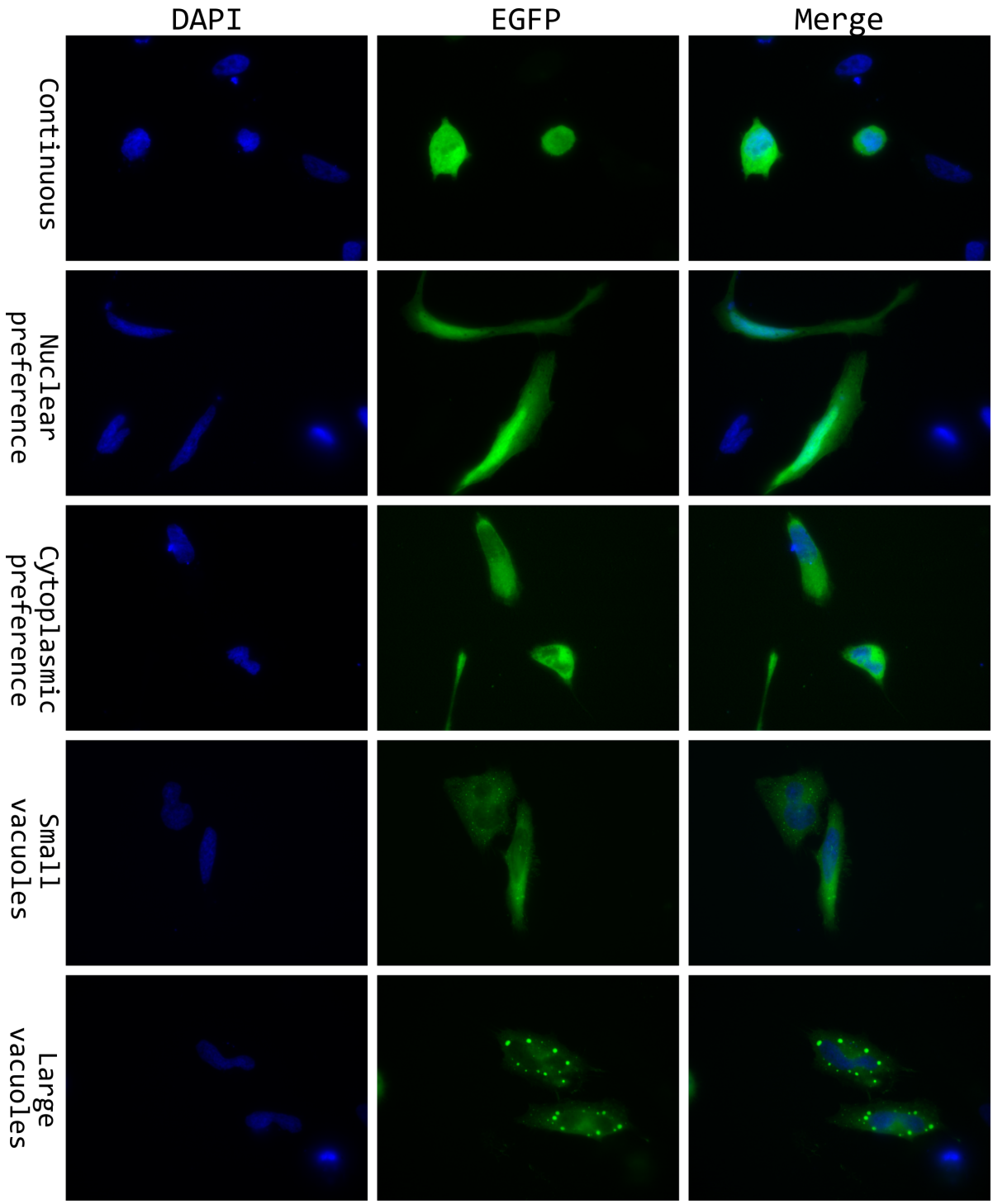

Figure 5.6: **Localisation patterns observed during cell counting.** HeLa cells were transfected with empty-EGFP, EGFP-p110β, or EGFP-Q68 containing plasmid (Table 3.8), then fixated, and labelled with DAPI, as a nuclear marker. Images were taken with a Leica DMI6000 B microscope (Table 3.5) at 1000× magnification. The five distinct phenotypes observed during cell counting are shown row by row, with the DAPI shown in the first, EGFP in the second, and the merge in the third column.

60% of the control cells showed an even distribution of EGFP in the cytoplasm, and nucleus, with the remaining EGFP expressing cells showing a nuclear preference for EGFP. Examples of these patterns are shown in figure 5.6, with the distribution shown in figure 5.7 B).

For the cells expressing EGFP-p110β, 50% showed an even distribution of EGFP signal within the cell (figure 5.7 A)). The second most observed pattern, at 29.8% (±7.6%) had a cytoplasmic preference for p110β. Two other patterns were observed for these cells, the largest population with 12.9% (±3.5%) had a pattern reminiscent of autophagy, with small cytoplasmic vacuoles. A similar pattern has been observed previously for p110β (Dou, Chattopadhyay, et al. 2010). The smallest population, with 7.4% (±3.7%), was similar, except that the observed vacuoles were significantly larger. Examples of each observed phenotype, are shown in figure 5.6, with the distribution shown in figure 5.7 B) with red bars.

For the Q68-EGFP, the largest population showed the small vacuoles, with 62.8% (±9.3%) of the observed cells having this pattern (5.7 B)). When compared to the EGFP-p110β transfected cells, about half as many, with 25.6% (±6.8%), had an even distribution of EGFP over the entire cell. With only 4.1% (±1.9%) showing a cytoplasmic preference. The percentage of cells showing the pattern were protein were aggregating to larger vacuoles was very similar to EGFP-p110β, with 7.4 % (±0.6%). Examples of each observed pattern, are shown in figure 5.6, with the distribution shown in figure 5.7 with yellow bars. If the small vacuoles are indeed indicative of autophagy activity, then it would seem that the shortform Q68 has greater autophagy activating effect than the canonical p110β form.

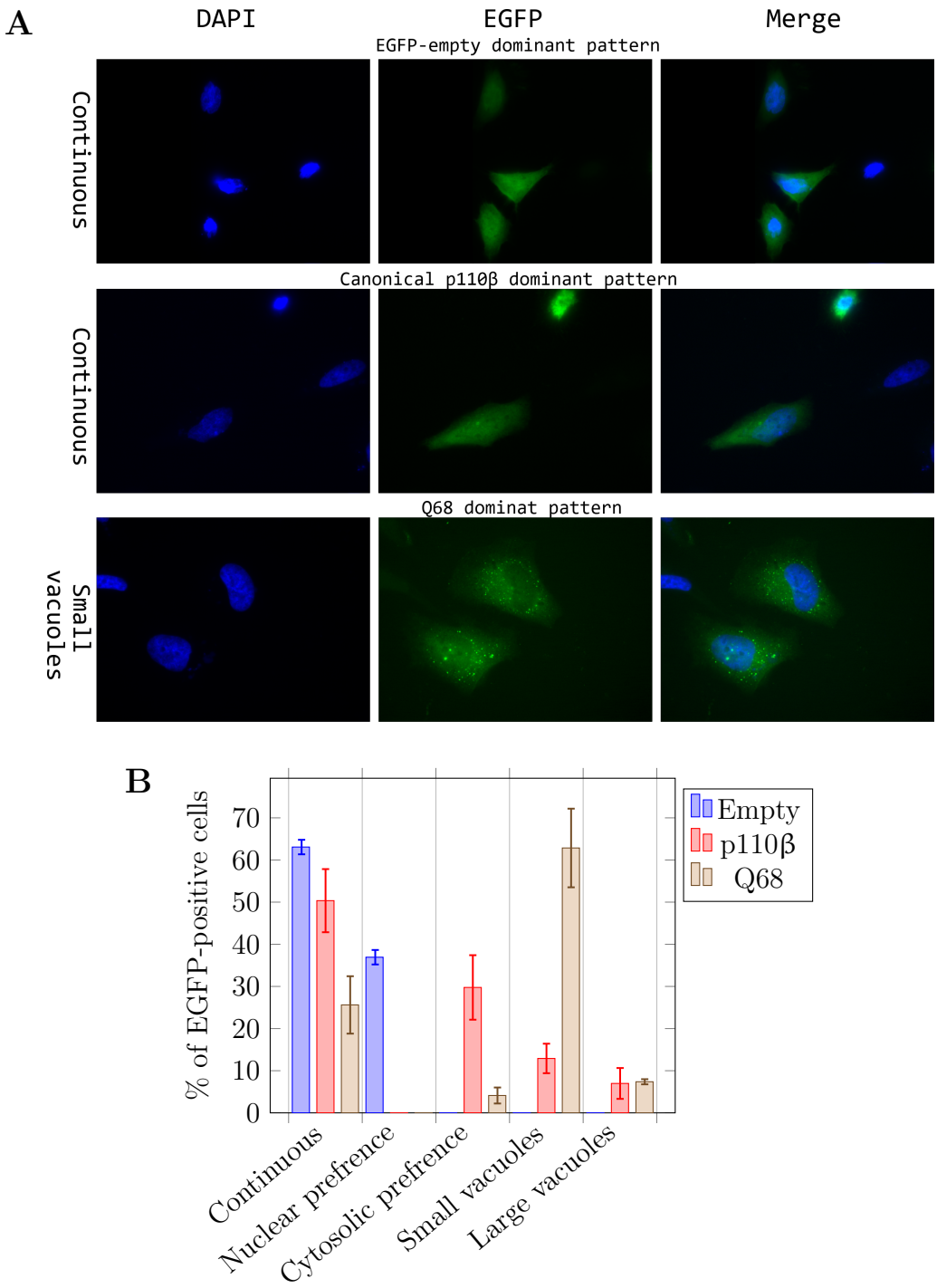

Figure 5.7: **p110β has a continuous domain pattern, while Q68 is cytoplasmic with intense small vacuoles dominant localisation pattern.** HeLa cells were transfected with EGFP as control, with EGFP-p110β, or EGFP-Q68. Cells were transfected for 24 h. The cells were then fixed, and stained with DAPI, as a nuclear marker. Images were taken with a Leica DMI6000 B microscope (Table 3.5) at 1000× magnification. Approximately 200 cells were imaged of each condition, in two transfections. **A)** The dominant pattern observed for EGFP-p110β, and EGFP-Q68 are shown. **C)** The quantification of the five distinct patterns observed during cell counting is shown in the graph. With the percentage of EGFP-positive cells expressing each pattern shown on the y-axis. The blue columns are cells transfected with EGFP, with the red and yellow columns representing cells transfected with p110β, and Q68 tagged with EGFP. Bars along the y-axis denote the standard deviation.

6 Discussion

The PI3K pathway is a complex interconnected reaction matrix, with extensive research conducted upon it. While much research has already been done, more still, remains to be uncovered about this pathway. Most research conducted upon the ubiquitously expressed Class I PI3Ks has been on p110α leaving the p110β PI3K as less understood. Our group, while working on other studies, found inconsistencies between experimental, and theoretical p110β resolving patterns in western blots. Discovering, and possibly explaining this inconsistency became the focus of this thesis.

During our work, it became more and more plausible that the theoretical isoform of p110β presented in Ensembl as "Q68DL0" correlated with the 50 kDa band observed in Thermo Fisher probed Western blots. Indeed it was found to be expressed in RL95-2 cells, at the mRNA level. It was also shown that the Q68 isoform contains a stronger Kozak sequence when compared to the canonical ATG. But other experiments we attempted have not been able to prove its existence as of yet.

6.1 Q68 may be a new short isoform of p110β translated from an alternative ATG.

The possibility of an alternative isoform for p110β was hinted at by the two antibodies, from Santa Cruz, and Thermo Fisher, and their differing western blot resolving patterns detected in whole, cytoplasmic, and nuclear fractions.

The most noticeable difference between the two anti-p110β antibodies was how the lower band, above 50 kDa, had apparent differing localization based on which antibody was used with the Thermo Fisher giving no signal in the cytoplasmic fraction, but a strong signal in the nuclear. While the Santa Cruz antibody gave a signal in the cytoplasmic fraction, but no such signal in the nuclear fraction.

Upon closer inspection, the 50 kDa band found in the Thermo Fisher blot in figure 5.1, is slightly lower than the Santa Cruz 50 kDa band, an observation made more evident by another member of our lab (non-published data). A possible explanation for this is that what we observe as the 50 kDa bands in these two blots maybe two different polypeptides; be that different degradation product(s), or possible isoform(s). If indeed the Q68 isoform exists then one would not expect the anti-p110β antibody from Santa Cruz to be able to bind to it, as its binding site (from AA: 2-31) is not present in the theoretical Q68. While

the antibody from Thermo Fisher may be able to bind to it, as parts of its binding site (from AA: 411-605)) is in the theoretical Q68 isoform (Figure 5.1). Still, it was not unlikely that both of these amino acid chains are degradation products, as p110β is an unstable protein, and may rapidly degrade when not stabilised by either its regulatory subunit or an N-terminal tag (Backer 2011).

The Q68 theoretical isoform was selected for further study as the most likely isoform to correlate with the 50 kDa band observed in figure 5.1 A). The expression of Q68 was tested for by conducting an RT-PCR experiment using primers that would bind to an insert found exclusively in the Q68 isoform. Designing a primer that would bind specifically to this insert turned out to be a challenge. We originally only designed one primer: 7591 (Table 3.6). While there were some possible unspecific annealing targets found for it during design, experimentally it did not bind to any of these targets in detectable levels. Two bands were detected and found to have high sequence identity with an unspecific protein, instead of the theoretical Q68 sequence.

Afterwards, we designed two new primers, trying to get a specific binding to the Q68 insert. 7495 was designed to anneal before, and in the entire insert, while 8001 was designed to anneal to before and after the insert. 7495 was also found to align with the same unspecific sequence as 7591 did, while 8001 only produced a sequence covering the Q68 insert, and 200 bp downstream of it.

Being able to sequence out the Q68 insert from RL95-2 cDNA, strongly suggests that Q68 is indeed expressed in WT cells, at least for RL95-2 cells. As this experiment was only conducted on RL95-2 cells, it remains to be seen if Q68 is expressed in other cell lines, or for that matter in living organisms. As far as we know, this isoform has not been characterised before, but further validation experiments are required.

Still, there is president for isoforms originating from downstream ATG's (dATG) (). It has also been shown that dATG's are more likely to be expressed in genes where the start ATG is located within a "suboptimal context", such as a weak Kozak sequence. Also, genes with suboptimal start ATG, and more optimal dATG' were found to contain longer 5′ UTRs, fitting the long 5′ UTR in *PIK3CB* (355 bp) (Bazykin and Kochetov 2011). Most isoforms starting from dATG do so within the first 50 codons, a gene starting 555 codons downstream is, as far as we know, undocumented.

We therefore, wanted to test if the Q68 isoform is translated from its predicted ATG site at AA 555 in p110β. This was tested for by conducting an experiment where either the canonical p110β or the theoretical Q68 isoform, had their ATG's mutated to AAC. If Q68

is expressed by the suspected ATG, then the band above 50 kDa should disappear only when this ATG is mutated. Another group have also used this method for the SPG4 gene, encoding spastin. This gene also contained a poor Kozak sequence at the start ATG, with a stronger Kozak at the dATG (Claudiani et al. 2005).

How successful we were at this experiment is arguable. While we did observe a similar pattern between the non-transfected sample, and the earlier probe on HeLa in figure 5.4 (Without the band bellow 100 kDa). The observations in the remaining samples were perplexing. While it is tempting to conclude the transfection itself a failure, there are some aspects that show that some transfection did take place. We have no reason to believe that the mutations were faulty as all of the mutations were confirmed by sequencing.

The most apparent oddity is that the bands we expected to be stronger in the transfection samples (above 100, and 50 kDa), are of the same intensity as the non-transfected sample. The transfected WT, even has a weaker band above 50 kDa, when compared to the control.

The next point is that both of the ATG mutants contained a band that we did not expect. The sample with the canonical ATG mutated still contains a band above 100 kDa. It is weaker than the 100 kDa bands in either WT and second ATG mutant, suggesting that this transfection did work to some extent. In any case, the Q68 ATG mutant sample is a bigger mystery. First: it contained a band at the Q68 location. Second: a band we have observed before (between 50, and 75 kDa), but not discussed, became stronger compared to the other samples. A similarly located band can also be observed in the nuclear load in figure 5.1 A, and in the whole fraction probed for both HEK and HeLa cell lines in figure 5.4.

A challenge during this experiment was that we could not check the transfection before probing on the western blot. This took us more time, and as a result,we had less time to perfect the protocols, and improve the transfection conditions.

So then what might have happened? Our main hypothesis to explain the weak transfection is that the transfection was not allowed to take place over a long enough time.

All in all, this experiment was only conducted once due to time constraints, and no honest conclusion can be extrapolated without conducting more transfections, and perfecting the protocol until repeatable transfection can be done.

6.2 Q68 is not nuclear, when overexpressed, with a bulky N-terminal tag.

Canonical p110β has already been shown to localize in the nucleus (Marqués et al. 2009). Our group has also previously found evidence of co-localization between p110β, and the nucleolus in several cell lines, including RL95-2, and AU565 cells (Gavgani, Morovicz, et al. 2020, and Karlsson et al. 2016). The nucleolus has been shown to, among other functions, produce most of the ribosomes within the cell (Derenzini, Montanaro, and Trerè 2017), making it vital for protein translation, and therefore cell proliferation. Nucleolar hypertrophy was even for some time considered as a diagnostic for malignancy; a theory that was discarded in the 20th century as normal cells undergoing cell proliferation was also found to exhibit nucleolar hypertrophy (Derenzini, Montanaro, and Trerè 2017). With the possible discovery of a new p110β isoform, the possibility of showing nucleolar localisation drove us to conduct a transfection experiment to show the localisation of overexpressed EGFP-tagged isoforms. The western blot in figure 5.1 A) showed nuclear localisation of the Thermo Fisher antibody target. We hypothesised that we would observe at least nuclear localisation for Q68, if not nucleolar. HeLa cells were transfected with canonical p110β, and shortform Q68 both tagged with EGFP on their N-terminus and made to overexpress these fusion proteins. The p110β was tagged at its N-terminus side specifically, as p110β is stabilised by bulky tags on the N-terminus (Backer 2011). We observed no nuclear, or nucleolar localisation for either the canonical or the Q68 isoform within the counted HeLa cells. Canonical p110β has been observed not to be transported to the nucleus when overexpressed (Kumar et al. 2011), and as such, the cytoplasmic localisation was expected for this form.

In contrast, our hypothesis for overexpressed Q68 placed its localisation within the nucleus. We expected this because of the probing with the Thermo Fisher p110β antibody showed nuclear localisation of the suspected Q68 band in figure 5.1 A). Our hypothesis was; that since Q68 can most likely not bind to the regulatory subunit p85 (at least as well as the canonical), as it does not contain the ABD domain, and it does not contain the suspected NLS (Kumar et al. 2011). That there would be other mechanisms separate from the canonical p110β's that would take over and shuttle the protein into the nucleus. Moreover, if this was the case, then we hoped that the Q68 would not have a similar overexpression pattern as the canonical p110β form. A possible explanation for the discrepancy is that EGFP is too big of a tag, changing the total mass of Q68 from 59.7 kDa to 86.6. Some proteins with mass less than approximately 50 kDa have been found to be shuttled into the nucleus without having an NLS or being reliant on co-transport (Cooper 2000). Tagging

Q68 with EGFP may have been enough to stop the transport of Q68 into the nucleus. In any case, Q68 can not translocate to the nucleus by itself, when overexpressed, and tagged to EGFP.

The use of a FLAG-tag may solve this problem, and should be considered for future experiments. FLAG-tags are polypeptide tags that can be fused our protein. These tags consist of a short specific polypeptide chain "DYKDDDDK" (Hopp et al. 1988), and would therefore not disturb the mass of Q68 to such an extent as EGFP does. A possible problem with this is that the stability of p110α is dependant on binding to either a regulatory subunit or on its fusion to a bulky N-terminal tag. The extent to stabilisation is also linear with the bulk of the N-terminal tag, with more bulky tags leading to higher stabilisation (Yu et al. 1998). We would expect p110β also exhibit this instability as the protein is structurally similar to p110α. The stabilising effect on p110β of FLAG would be lower when compared to EGFP. An alternative solution would be to incubate the cells at a lower temperature such as 30℃; this temperature has been shown to imitate the stabilising effect of the regulatory subunit on p110α (Yu et al. 1998). This may induce a change in expression in the cells due to stress. Another solution would be to tag p110β with a bulky N-terminal tag and fuse the flag tag at the C-terminus instead, stabilizing the protein, while still allowing detection by FLAG. Lastly, the regulatory subunit could be overexpressed at the same time, and act to stabilize p110β.

6.3 Q68 may have a stronger connection to autophagy than p110β, in HeLa cells

The dominant pattern we did observe for Q68 was a strong tendency to segregate to apparent small vacuoles reminiscent of the pattern observed for p110β when active in autophagy (Dou, Chattopadhyay, et al. 2010, and Dou, Pan, et al. 2013). These vacuoles appeared as small specs, distributed evenly within the cytoplasm. It is possible that Q68 functions much the same as the canonical p110β is hypothesised to do. As discussed earlier, the canonical p110β has been observed to have a possible regulatory role for autophagy, allowing multicellular organisms to initiate autophagy by limiting growth signals, instead of just being initiated by limited nutrient availability (Dou, Pan, et al. 2013).

The binding between p110β and Rab5 has been found to be reliant on two amino acids, Q596, and I597S (Dou, Pan, et al. 2013). Q68 contains these amino acids, and it is, therefore, possible that Q68 can also bind to Rab5, and act as a scaffolding protein as p110β does.

The strong correlation between Q68, and the apparent autophagy pattern, hints at a possible function for this isoform as autophagy initiating/promoting molecule.

A problem with this hypothesis is that, as mentioned, the autophagy role ofp110β is controversial (Bresnick and Backer 2019). One of the controversial points is that Rab5, is expressed at 150 times more, then p110β in vivo (Schwanhäusser et al. 2011), making it unlikely that p110β can function on Rab5, in a discernible manner. The same argument can also be used for Q68, to a more significant effect even. While we have not quantified the expression levels of Q68, the weaker bands, and general difficulty of detecting this isoform are good indicators that the short isoform, is expressed at lower levels then canonical p110β.

6.4 Which band does represent Q68?

The band briefly touched on in the previous section, the one sometimes found above what we believe to be Q68, and bellow the 75 kDa marker, has made us unsure if we have constituted as the Q68, *is* the Q68 band. For one Q68, has a theoretical mass of 59'770 Da. It might be that the band above 50 kDa found during probing using the Thermo Fisher antibody is too low to represent the Q68 isoform, and instead, the higher is representative of Q68.

This theory is supported by the pattern shown by the WT p110β Kozak in figure 5.1, where the band above 50 kDa is not visible, while the band bellow 75 kDa is. If the band bellow 75 kDa represents Q68, then that would mean that the overexpression made it visible. Contradicting this observation is the fact that the band bellow 75 kDa is equally strong in the WT, as in the Q68 ATG mutant samples in figure 5.5. If there was a mix up during loading of the ATG mutants, and the actual samples are opposite, i.e. "1st ATG mutant" is the "2nd ATG mutant", and inversely for the other mutant. Then the bellow 75 kDa band may represent the Q68 isoform. Otherwise, it becomes unlikely. We find the possibility of a mix up as unlikely, but not impossible. Due to time constrains two, people handled the mutant during SDM, and a mix-up might have happened at some point during this process. Sequencing the samples, and clearing the possibility of this error should be done before repeating the experiment. The possibility of the bellow 75 kDa band being the Q68 is also supported for in figure 4.1 A, where a befitting band can be observed in the nuclear sample. Inversely, this band can also be a degradation product of canonical p110β. That becomes more visible when the canonical form is overexpressed.

The band bellow 75 kDa may also be explained by another dATG. Three in-frame codons are possible candidates at AA-444 (ATACG<u>ATG</u>GTT), 472 (AAGAA<u>ATG</u>TTG), and 476

(ATCCAATGGGA). On the basis on matching the band observed bellow 75kDa the codons at AA-472, and 476 fit best based on mass, with theoretical masses of 69.1 kDa, and 68.6 kDa. That said the dATG at AA-444 contains the strongest Kozak signal ($CC\underset{G}{A}CC\mathbf{ATG}\underline{G}GC$), containing both the -3 and +1 most conserved bases. The other two codons are only surrounded by one of these conserved bases. By surveying the data-set collected by (Philippon, Brochier-Armanet, and Perrière 2015), it was found that all of these dATGs have conserved Kozak sequences in the *PIK3CB* gene over the entire Amniota clade. Of the conserved dATGs the AA-444, and AA-472 were also found to be conserved in all of the species of the Osteichthyes clade. Q68's theoretical ATG is conserved for all of the members in the Amniota clade. One outlier was the Latimeria *chalumnae* (Philippon, Brochier-Armanet, and Perrière 2015). This may be indicative of the importance of the Kozak sequence for one of these ATG's. Of note is all of the dATG's are found within the helical domain, which itself is conserved (Philippon, Brochier-Armanet, and Perrière 2015). The conservation of the dATG's may therefore be a consequence of the helical domain, not the Q68 expression.

In conclusion, our findings establish the novel "Q68" sequence as a possible p110β isoform, based on detecting a specific mRNA sequence, and describing an alternative start codon surrounded by a strong Kozak sequence. These preliminary findings motivate further studies into the possible existence, and function of this elusive protein. The discovery of an alternative p110β isoform may explain some aspects of p110β which are currently not known, or not understood well. For example, the possible correlation between p110β and autophagy. Future experiments might include alternative overexpression experiments, in order to solve the apparent localisation discrepancy between Western blot probing, and overexpression by transfection. Solving the ATG mutation experiment could also elucidate the uncertainty of the alternative ATG.

References

Aoki, M. et al. (2000). "The catalytic subunit of phosphoinositide 3-kinase: requirements for oncogenicity". In: *The Journal of Biological Chemistry* 275.9, pp. 6267–6275. DOI: 10.1074/jbc.275.9.6267.

Backer, Jonathan M. (2008). "The regulation and function of Class III PI3Ks: novel roles for Vps34". In: *Biochemical Journal* 410.1. Publisher: Portland Press, pp. 1–17. DOI: 10.1042/BJ20071427.

— (2011). "The Regulation of Class IA PI 3-Kinases by Inter-Subunit Interactions". In: *Phosphoinositide 3-kinase in Health and Disease: Volume 1*. Ed. by Christian Rommel, Bart Vanhaesebroeck, and Peter K. Vogt. Current Topics in Microbiology and Immunology. Berlin, Heidelberg: Springer, pp. 87–114. DOI: 10.1007/82_2010_52.

Bazykin, Georgii A. and Alex V. Kochetov (2011). "Alternative translation start sites are conserved in eukaryotic genomes". In: *Nucleic Acids Research* 39.2, pp. 567–577. DOI: 10.1093/nar/gkq806.

Berenjeno, Inma M. et al. (2012). "Both p110α and p110β isoforms of PI3K can modulate the impact of loss-of-function of the PTEN tumour suppressor". In: *Biochemical Journal* 442 (Pt 1), pp. 151–159. DOI: 10.1042/BJ20111741.

Bi, L., I. Okabe, D. J. Bernard, A. Wynshaw-Boris, et al. (1999). "Proliferative defect and embryonic lethality in mice homozygous for a deletion in the p110alpha subunit of phosphoinositide 3-kinase". In: *The Journal of Biological Chemistry* 274.16, pp. 10963–10968. DOI: 10.1074/jbc.274.16.10963.

Bi, Lei, Ichiro Okabe, David J. Bernard, and Robert L. Nussbaum (2002). "Early embryonic lethality in mice deficient in the p110beta catalytic subunit of PI 3-kinase". In: *Mammalian Genome: Official Journal of the International Mammalian Genome Society* 13.3, pp. 169–172. DOI: 10.1007/BF02684023.

Bresnick, Anne R. and Jonathan M. Backer (2019). "PI3Kβ—A Versatile Transducer for GPCR, RTK, and Small GTPase Signaling". In: *Endocrinology* 160.3. Publisher: Oxford Academic, pp. 536–555. DOI: 10.1210/en.2018-00843.

Burke, John E. and Roger L. Williams (2015). "Synergy in activating class I PI3Ks". In: *Trends in Biochemical Sciences* 40.2, pp. 88–100. DOI: 10.1016/j.tibs.2014.12.003.

Chamberlain, M. Dean et al. (2004). "The p85alpha subunit of phosphatidylinositol 3'-kinase binds to and stimulates the GTPase activity of Rab proteins". In: *The Journal of Biological Chemistry* 279.47, pp. 48607–48614. DOI: 10.1074/jbc.M409769200.

Chang, Matthew T. et al. (2016). "Identifying recurrent mutations in cancer reveals widespread lineage diversity and mutational specificity". In: *Nature Biotechnology* 34.2, pp. 155–163. DOI: 10.1038/nbt.3391.

Ciraolo, Elisa et al. (2008). "Phosphoinositide 3-kinase p110beta activity: key role in metabolism and mammary gland cancer but not development". In: *Science Signaling* 1.36, ra3. DOI: 10.1126/scisignal.1161577.

Claudiani, Pamela et al. (2005). "Spastin subcellular localization is regulated through usage of different translation start sites and active export from the nucleus". In: *Experimental Cell Research* 309.2, pp. 358–369. DOI: 10.1016/j.yexcr.2005.06.009.

Cocco, L. et al. (1987). "Synthesis of polyphosphoinositides in nuclei of Friend cells. Evidence for polyphosphoinositide metabolism inside the nucleus which changes with cell differentiation". In: *The Biochemical Journal* 248.3, pp. 765–770. DOI: 10.1042/bj2480765.

Cooper, Geoffrey M. (2000). "The Nuclear Envelope and Traffic between the Nucleus and Cytoplasm". In: *The Cell: A Molecular Approach. 2nd edition.* Publisher: Sinauer Associates.

Cosmic (2020). *PIK3CA Hallmarks of Cancer*. URL: https://cancer.sanger.ac.uk/cosmic/census-page/PIK3CA (visited on 11/19/2020).

Davis, William J., Peter Z. Lehmann, and Weimin Li (2015). "Nuclear PI3K signaling in cell growth and tumorigenesis". In: *Frontiers in Cell and Developmental Biology* 3. DOI: 10.3389/fcell.2015.00024.

Dbouk, Hashem A. et al. (2013). "Characterization of a Tumor-Associated Activating Mutation of the p110β PI 3-Kinase". In: *PLOS ONE* 8.5. Publisher: Public Library of Science, e63833. DOI: 10.1371/journal.pone.0063833.

Derenzini, Massimo, Lorenzo Montanaro, and Davide Trerè (2017). "Ribosome biogenesis and cancer". In: *Acta Histochemica* 119.3, pp. 190–197. DOI: 10.1016/j.acthis.2017.01.009.

Dou, Zhixun, Mohar Chattopadhyay, et al. (2010). "The class IA phosphatidylinositol 3-kinase p110-beta subunit is a positive regulator of autophagy". In: *The Journal of Cell Biology* 191.4, pp. 827–843. DOI: 10.1083/jcb.201006056.

Dou, Zhixun, Ji-An Pan, et al. (2013). "Class IA PI3K p110β Subunit Promotes Autophagy through Rab5 Small GTPase in Response to Growth Factor Limitation". In: *Molecular Cell* 50.1, pp. 29–42. DOI: 10.1016/j.molcel.2013.01.022.

Farah, Carole and Wayne Sossin (2012). "The role of C2 domains in PKC signaling". In: *Advances in experimental medicine and biology* 740, pp. 663–83. DOI: 10.1007/978-94-007-2888-2_29.

Fiume, R. et al. (2019). "Nuclear Phosphoinositides: Their Regulation and Roles in Nuclear Functions". In: *International Journal of Molecular Sciences* 20.12. DOI: 10.3390/ijms20122991.

Flinn, Rory J. et al. (2010). "The late endosome is essential for mTORC1 signaling". In: *Molecular Biology of the Cell* 21.5, pp. 833–841. DOI: 10.1091/mbc.e09-09-0756.

Fritsch, Ralph et al. (2013). "RAS and RHO Families of GTPases Directly Regulate Distinct Phosphoinositide 3-Kinase Isoforms". In: *Cell* 153.5, pp. 1050–1063. DOI: 10.1016/j.cell.2013.04.031.

Fruman, David A. and Christian Rommel (2014). "PI3K and Cancer: Lessons, Challenges and Opportunities". In: *Nature reviews. Drug discovery* 13.2, pp. 140–156. DOI: 10.1038/nrd4204.

Gavgani, Fatemeh Mazloumi, Thomas Karlsson, et al. (2019). "Nuclear upregulation of PI3K p110β correlates with increased rRNA transcription in endometrial cancer cells". In: *bioRxiv*. Publisher: Cold Spring Harbor Laboratory Section: New Results, p. 2019.12.20.884122. DOI: 10.1101/2019.12.20.884122.

Gavgani, Fatemeh Mazloumi, Andrea Papdiné Morovicz, et al. (2020). "Nuclear phosphatidylinositol 3,4,5-trisphosphate interactome uncovers an enrichment in nucleolar proteins". In: *bioRxiv*. Publisher: Cold Spring Harbor Laboratory Section: New Results, p. 2020.05.17.100446. DOI: 10.1101/2020.05.17.100446.

Gene: PIK3CB - Ensembl (2020). URL: https://www.ensembl.org/Homo_sapiens/Gene/Summary?db=core;g=ENSG00000051382;r=3:138652698-138834928 (visited on 12/01/2020).

Gerace, L., A. Blum, and G. Blobel (1978). "Immunocytochemical localization of the major polypeptides of the nuclear pore complex-lamina fraction. Interphase and mitotic distribution". In: *The Journal of Cell Biology* 79.2, pp. 546–566. DOI: 10.1083/jcb.79.2.546.

Hamann, Bree L. and Raymond D. Blind (2018). "Nuclear phosphoinositide regulation of chromatin". In: *Journal of Cellular Physiology* 233.1, pp. 107–123. DOI: 10.1002/jcp.25886.

Hanahan, Douglas and Robert A. Weinberg (2000). "The Hallmarks of Cancer". In: *Cell* 100.1. Publisher: Elsevier, pp. 57–70. DOI: 10.1016/S0092-8674(00)81683-9.

— (2011). "Hallmarks of Cancer: The Next Generation". In: *Cell* 144.5. Publisher: Elsevier, pp. 646–674. DOI: 10.1016/j.cell.2011.02.013.

Hiles, Ian D. et al. (1992). "Phosphatidylinositol 3-kinase: Structure and expression of the 110 kd catalytic subunit". In: *Cell* 70.3, pp. 419–429. DOI: 10.1016/0092-8674(92)90166-A.

Hill, Karren M et al. (2010). "The role of PI 3-kinase p110beta in AKT signally, cell survival, and proliferation in human prostate cancer cells." In: *The Prostate* 70.7, pp. 755–764. DOI: 10.1002/pros.21108.

Hopkins, Benjamin D. et al. (2014). "PTEN function, the long and the short of it". In: *Trends in biochemical sciences* 39.4, pp. 183–190. DOI: 10.1016/j.tibs.2014.02.006.

Hopp, Thomas P. et al. (1988). "A Short Polypeptide Marker Sequence Useful for Recombinant Protein Identification and Purification". In: *Bio/Technology* 6.10. Number: 10 Publisher: Nature Publishing Group, pp. 1204–1210. DOI: 10.1038/nbt1088-1204.

Hu, P et al. (1993). "Cloning of a novel, ubiquitously expressed human phosphatidylinositol 3-kinase and identification of its binding site on p85." In: *Molecular and Cellular Biology* 13.12, pp. 7677–7688.

Huang, Bill X. et al. (2011). "Phosphatidylserine is a critical modulator for Akt activation". In: *Journal of Cell Biology* 192.6. Publisher: The Rockefeller University Press, pp. 979–992. DOI: 10.1083/jcb.201005100.

Irvine, Robin F. (2003). "Nuclear lipid signalling". In: *Nature Reviews Molecular Cell Biology* 4.5. Number: 5 Publisher: Nature Publishing Group, pp. 349–361. DOI: 10.1038/nrm1100.

Jaber, Nadia and Wei-Xing Zong (2013). "Class III PI3K Vps34: essential roles in autophagy, endocytosis, and heart and liver function". In: *Annals of the New York Academy of Sciences* 1280, pp. 48–51. DOI: 10.1111/nyas.12026.

Jacobsen, Rhian Gaenor et al. (2019). "Polyphosphoinositides in the nucleus: Roadmap of their effectors and mechanisms of interaction". In: *Advances in Biological Regulation*. Accepted: 2020-08-07T11:33:51Z Publisher: Elsevier. DOI: 10.1016/j.jbior.2019.04.001.

Jean, Steve and Amy A. Kiger (2014). "Classes of phosphoinositide 3-kinases at a glance". In: *Journal of Cell Science* 127.5, pp. 923–928. DOI: 10.1242/jcs.093773.

Jia, Shidong et al. (2008). "Essential roles of PI(3)K-p110beta in cell growth, metabolism and tumorigenesis". In: *Nature* 454.7205, pp. 776–779. DOI: 10.1038/nature07091.

Kan, Zhengyan et al. (2010). "Diverse somatic mutation patterns and pathway alterations in human cancers". In: *Nature* 466.7308. Number: 7308 Publisher: Nature Publishing Group, pp. 869–873. DOI: 10.1038/nature09208.

Kang, Sohye, Andreas G. Bader, and Peter K. Vogt (2005). "Phosphatidylinositol 3-kinase mutations identified in human cancer are oncogenic". In: *Proceedings of the National Academy of Sciences of the United States of America* 102.3, pp. 802–807. DOI: 10.1073/pnas.0408864102.

Karlsson, Thomas et al. (2016). "Endometrial cancer cells exhibit high expression of p110β and its selective inhibition induces variable responses on PI3K signaling, cell survival and proliferation". In: *Oncotarget* 8.3, pp. 3881–3894. DOI: 10.18632/oncotarget.13989.

Kihara, Akio et al. (2001). "Two Distinct Vps34 Phosphatidylinositol 3–Kinase Complexes Function in Autophagy and Carboxypeptidase Y Sorting inSaccharomyces cerevisiae". In: *The Journal of Cell Biology* 152.3, pp. 519–530.

Kozak, Marilyn (1989). "The scanning model for translation: an update". In: *The Journal of Cell Biology* 108.2, pp. 229–241.

Kumar, Amit et al. (2011). "Nuclear but Not Cytosolic Phosphoinositide 3-Kinase Beta Has an Essential Function in Cell Survival". In: *Molecular and Cellular Biology* 31.10, pp. 2122–2133. DOI: 10.1128/MCB.01313-10.

Lachyankar, M. B. et al. (2000). "A role for nuclear PTEN in neuronal differentiation". In: *The Journal of Neuroscience: The Official Journal of the Society for Neuroscience* 20.4, pp. 1404–1413.

Lasota, Jerzy et al. (2019). "New Mechanisms of mTOR Pathway Activation in KIT-mutant Malignant GISTs". In: *Applied immunohistochemistry & molecular morphology: AIMM* 27.1, pp. 54–58. DOI: 10.1097/PAI.0000000000000541.

Leevers, S. J., B. Vanhaesebroeck, and M. D. Waterfield (1999). "Signalling through phosphoinositide 3-kinases: the lipids take centre stage". In: *Current Opinion in Cell Biology* 11.2, pp. 219–225. DOI: 10.1016/S0955-0674(99)80029-5.

Levine, Beth and Guido Kroemer (2008). "Autophagy in the pathogenesis of disease". In: *Cell* 132.1, pp. 27–42. DOI: 10.1016/j.cell.2007.12.018.

Levine, Beth and Junying Yuan (2005). "Autophagy in cell death: an innocent convict?" In: *The Journal of Clinical Investigation* 115.10, pp. 2679–2688. DOI: 10.1172/JCI26390.

Li, J. et al. (1997). "PTEN, a putative protein tyrosine phosphatase gene mutated in human brain, breast, and prostate cancer". In: *Science (New York, N.Y.)* 275.5308, pp. 1943–1947. DOI: 10.1126/science.275.5308.1943.

Lum, Julian J., Ralph J. DeBerardinis, and Craig B. Thompson (2005). "Autophagy in metazoans: cell survival in the land of plenty". In: *Nature Reviews. Molecular Cell Biology* 6.6, pp. 439–448. DOI: 10.1038/nrm1660.

Marqués, Miriam et al. (2009). "Specific function of phosphoinositide 3-kinase beta in the control of DNA replication". In: *Proceedings of the National Academy of Sciences*. Publisher: National Academy of Sciences Section: Biological Sciences. DOI: 10.1073/pnas.0812000106.

Martelli, Alberto et al. (2011). "Nuclear phosphoinositides and their roles in cell biology and disease". In: *Critical reviews in biochemistry and molecular biology* 46, pp. 436–57. DOI: 10.3109/10409238.2011.609530.

Musille, Paul M., Jeffrey A. Kohn, and Eric A. Ortlund (2013). "Phospholipid–driven gene regulation". In: *FEBS letters* 587.8, pp. 1238–1246. DOI: 10.1016/j.febslet.2013.01.004.

Nakanishi, Yoshito et al. (2016). "Activating Mutations in PIK3CB Confer Resistance to PI3K Inhibition and Define a Novel Oncogenic Role for p110β". In: *Cancer Research* 76.5, pp. 1193–1203. DOI: 10.1158/0008-5472.CAN-15-2201.

Okada, Masashi and Keqiang Ye (2009). "Nuclear phosphoinositide signaling regulates messenger RNA export". In: *RNA Biology* 6.1. Publisher: Taylor & Francis _eprint: https://doi.org/10.4161/rna.6.1.7439, pp. 12–16. DOI: 10.4161/rna.6.1.7439.

Osborne, S. L. et al. (2001). "Nuclear PtdIns(4,5)P2 assembles in a mitotically regulated particle involved in pre-mRNA splicing". In: *Journal of Cell Science* 114 (Pt 13), pp. 2501–2511.

Payrastre, B. et al. (1992). "A differential location of phosphoinositide kinases, diacylglycerol kinase, and phospholipase C in the nuclear matrix". In: *The Journal of Biological Chemistry* 267.8, pp. 5078–5084.

Pazarentzos, E. et al. (2016). "Oncogenic activation of the PI3-kinase p110β isoform via the tumor-derived PIK3Cβ(D1067V) kinase domain mutation". In: *Oncogene* 35.9, pp. 1198–1205. DOI: 10.1038/onc.2015.173.

Philippon, Héloïse, Céline Brochier-Armanet, and Guy Perrière (2015). "Evolutionary history of phosphatidylinositol- 3-kinases: ancestral origin in eukaryotes and complex duplication patterns". In: *BMC Evolutionary Biology* 15. DOI: 10.1186/s12862-015-0498-7.

PI 3-kinase p110β Antibody (C-8) (2020). URL: https://www.scbt.com/p/pi-3-kinase-p110beta-antibody-c-8 (visited on 10/15/2020).

PIK helical domain - PRU00878 (2020). URL: https://prosite.expasy.org/rule/PRU00878 (visited on 11/26/2020).

PIK3CB - Phosphatidylinositol 4,5-bisphosphate 3-kinase catalytic subunit beta isoform - Homo sapiens (Human) - PIK3CB gene & protein (2020). URL: https://www.uniprot.org/uniprot/Q68DL0 (visited on 10/15/2020).

PIK3CB Antibody (703364) (2020). URL: https://www.thermofisher.com/antibody/product/PIK3CB-Antibody-clone-1H9L37-Recombinant-Monoclonal/703364 (visited on 10/15/2020).

Posor, York, Marielle Eichhorn-Grünig, and Volker Haucke (2015). "Phosphoinositides in endocytosis". In: *Biochimica Et Biophysica Acta* 1851.6, pp. 794–804. DOI: 10.1016/j.bbalip.2014.09.014.

Redondo-Muñoz, Javier, María Josefa Rodríguez, et al. (2013). "Phosphoinositide 3-kinase beta controls replication factor C assembly and function". In: *Nucleic Acids Research* 41.2. Publisher: Oxford Academic, pp. 855–868. DOI: 10.1093/nar/gks1095.

Redondo-Muñoz, Javier, Vicente Pérez-García, et al. (2015). "Phosphoinositide 3-Kinase Beta Protects Nuclear Envelope Integrity by Controlling RCC1 Localization and Ran Activity". In: *Molecular and Cellular Biology* 35.1, pp. 249–263. DOI: 10.1128/MCB.01184-14.

Robinson, Dan et al. (2015). "Integrative clinical genomics of advanced prostate cancer". In: *Cell* 161.5, pp. 1215–1228. DOI: 10.1016/j.cell.2015.05.001.

Rodriguez-Viciana, P. et al. (1996). "Activation of phosphoinositide 3-kinase by interaction with Ras and by point mutation". In: *The EMBO journal* 15.10, pp. 2442–2451.

Sarbassov, Dos D. et al. (2005). "Phosphorylation and Regulation of Akt/PKB by the Rictor-mTOR Complex". In: *Science* 307.5712. Publisher: American Association for the Advancement of Science Section: Report, pp. 1098–1101. DOI: 10.1126/science.1106148.

Schwanhäusser, Björn et al. (2011). "Global quantification of mammalian gene expression control". In: *Nature* 473.7347, pp. 337–342. DOI: 10.1038/nature10098.

Silió, Virginia, Javier Redondo-Muñoz, and Ana C. Carrera (2012). "Phosphoinositide 3-kinase β regulates chromosome segregation in mitosis". In: *Molecular Biology of the Cell* 23.23, pp. 4526–4542. DOI: 10.1091/mbc.E12-05-0371.

Steck, P. A. et al. (1997). "Identification of a candidate tumour suppressor gene, MMAC1, at chromosome 10q23.3 that is mutated in multiple advanced cancers". In: *Nature Genetics* 15.4, pp. 356–362. DOI: 10.1038/ng0497-356.

Thorpe, Lauren M., Haluk Yuzugullu, and Jean J. Zhao (2015). "PI3K in cancer: divergent roles of isoforms, modes of activation, and therapeutic targeting". In: *Nature reviews. Cancer* 15.1, pp. 7–24. DOI: 10.1038/nrc3860.

Transcript flags (2020). URL: https://grch37.ensembl.org/info/genome/genebuild/transcript_quality_tags.html (visited on 10/13/2020).

Vanhaesebroeck, B. and M. D. Waterfield (1999). "Signaling by distinct classes of phosphoinositide 3-kinases". In: *Experimental Cell Research* 253.1, pp. 239–254. DOI: 10.1006/excr.1999.4701.

Viaud, Julien et al. (2016). "Phosphoinositides: Important lipids in the coordination of cell dynamics". In: *Biochimie* 125, pp. 250–258. DOI: 10.1016/j.biochi.2015.09.005.

Viiri, Keijo, Markku Mäki, and Olli Lohi (2012). "Phosphoinositides as Regulators of Protein-Chromatin Interactions". In: *Science Signaling* 5.222. Publisher: American Association for the Advancement of Science Section: Perspective, pe19–pe19. DOI: 10.1126/scisignal.2002917.

Watt, Stephen A et al. (2002). "Subcellular localization of phosphatidylinositol 4,5-bisphosphate using the pleckstrin homology domain of phospholipase C delta1." In: *Biochemical Journal* 363 (Pt 3), pp. 657–666.

Yang, Jing et al. (2019). "Targeting PI3K in cancer: mechanisms and advances in clinical trials". In: *Molecular Cancer* 18.1, p. 26. DOI: 10.1186/s12943-019-0954-x.

Yu, Jinghua et al. (1998). "Regulation of the p85/p110 Phosphatidylinositol 3′-Kinase: Stabilization and Inhibition of the p110α Catalytic Subunit by the p85 Regulatory Subunit". In: *Molecular and Cellular Biology* 18.3, pp. 1379–1387. DOI: 10.1128/MCB.18.3.1379.

Zhao, Li and Peter K. Vogt (2008). "Helical domain and kinase domain mutations in p110α of phosphatidylinositol 3-kinase induce gain of function by different mechanisms". In: *Proceedings of the National Academy of Sciences* 105.7. ISBN: 9780712169103 Publisher: National Academy of Sciences Section: Biological Sciences, pp. 2652–2657. DOI: 10.1073/pnas.0712169105.

Appendix

6.5 RNA extraction

Harvesting cells for RNA isolation was generally done in 1× 15 cm plate of 80% confluent cells. When different culture plates were used, volumes were adjusted proportionally. Media was removed, and cells were washed once with PBS before completely trypsinizing and collecting into a tube. This was followed by centrifuging at 70 ×g for 5 min and kept on ice.

Media was removed, and the pellet was carefully washed with 5 mL PBS and centrifuged at 300 ×g for 5 min at 4℃. The cell pellet was resuspended in 1 mL of PBS, and centrifuged at 300 ×g for 5 min at 4℃. PBS was discarded, and the previous centrifugation step was repeated, but for 1 min to remove excess PBS. The pellet was carefully resuspended in 1 mL TRI reagent (TRI Reagent®, Sigma-Aldrich, T9424), and incubated at RT for 5-10 min, and frozen at -80℃ until needed.

For RNA isolation, all steps were performed at RT, unless otherwise specified. Cells resuspended in TRI reagent were thawed, to which 200 µl chloroform was added. The contents were vortexed for 1 min, then again for 30 sec, before being incubated for 1 min and centrifuged at 12'000 ×g for 15 min at 4℃. The top layer was transferred and placed on ice, to which 500 µl phenol chloroform isoamyl alcohol mixture was added on ice. Contents were vortexed for 1 min and incubated for 2 min, then centrifuged at 12'000 ×g for 10 min at 4℃. Again, the top layer was transferred on ice, and 500 µl chloroform was added, vortexed for 1 min and incubated for 1 min, then centrifuged at 12'000 ×g for 10 min at 4℃. Top phase was collected on ice, and 20 µg of RNA grade glycogen was added along with 500 µl isopropanol, before vortexing for 10 sec, and incubating for 20-30min. After incubation, the solution was centrifuged at 13'000 ×g for 20 min at 4℃, and supernatant was discarded. Pellet was resuspended in 1 mL ice-cold 70% ethanol, vortexed for 30 sec, and centrifuged at 8000 ×g for 5 min at 4℃. Supernatant was discarded, and pellet was spun down at 8000 ×g for 5 min at 4℃ to remove any ethanol. RNase free water was added to the pellet (volume depending on pellet size), and vortexed for 5 sec every 5 min for 20 min. RNA concentration was measured in an Epoch microplate Spectrophotometer, and total RNA was stored in -80℃ until needed.

6.6 cDNA synthesis

1 µg of total RNA was used to produce 50 ng/µl cDNA with random primers according to the protocol given in the High-Capacity cDNA Reverse Transcription Kit. Transcribed cDNA was stored at -20℃ until real-time PCR (RT-PCR) was run.

6.7 TSL score

Show/hide columns (1 hidden) Filter

Name	Transcript ID	bp	Protein	Biotype	CCDS	UniProt	RefSeq Match	Flags
PIK3CB-214	ENST00000674063.1	6259	1070aa	Protein coding	CCDS3104	-	NM_006219.3	GENCODE basic APPRIS P1 MANE Select v0.9
PIK3CB-201	ENST00000289153.6	5919	1070aa	Protein coding	CCDS3104	P42338	-	TSL:1 GENCODE basic APPRIS P1
PIK3CB-207	ENST00000477593.5	4658	1070aa	Protein coding	CCDS3104	P42338	-	TSL:5 GENCODE basic APPRIS P1
PIK3CB-212	ENST00000493568.5	2347	702aa	Protein coding	-	H0Y871	-	CDS 5' incomplete TSL:2
PIK3CB-213	ENST00000544716.5	3181	521aa	Protein coding	-	Q68DL0	-	TSL:1 GENCODE basic
PIK3CB-206	ENST00000473435.1	904	245aa	Nonsense mediated decay	-	H7C565	-	CDS 5' incomplete TSL:5
PIK3CB-202	ENST00000462294.1	542	181aa	Protein coding	-	H7C527	-	CDS 5' and 3' incomplete TSL:5
PIK3CB-203	ENST00000462898.5	4747	134aa	Nonsense mediated decay	-	F8WDJ8	-	TSL:5
PIK3CB-209	ENST00000483968.5	721	131aa	Protein coding	-	C9JYX0	-	CDS 3' incomplete TSL:3
PIK3CB-204	ENST00000465581.1	690	56aa	Protein coding	-	C9J345	-	CDS 3' incomplete TSL:3
PIK3CB-205	ENST00000469284.6	3164	34aa	Nonsense mediated decay	-	H7C5C3	-	CDS 5' incomplete TSL:5
PIK3CB-208	ENST00000481749.5	2396	No protein	Retained intron	-	-	-	TSL:2
PIK3CB-210	ENST00000485060.1	612	No protein	Retained intron	-	-	-	TSL:3
PIK3CB-211	ENST00000487552.1	581	No protein	Retained intron	-	-	-	TSL:2

Figure 6.1: **Screenshot of ensambl page for the PIK3CB gene showing only the canonical (P42338), and the Q68DL0 forms with a TSL score of 1.**